



**HAL**  
open science

## A supernumerary “B-sex” chromosome drives male sex determination in the Pachón cavefish, *Astyanax mexicanus*

Boudjema Imarazene, Kang Du, Séverine Beille, Elodie Jouanno, Romain Feron, Qiaowei Pan, Jorge Torres-Paz, Céline Lopez-Roques, Adrien Castinel, Lisa Gil, et al.

### ► To cite this version:

Boudjema Imarazene, Kang Du, Séverine Beille, Elodie Jouanno, Romain Feron, et al.. A supernumerary “B-sex” chromosome drives male sex determination in the Pachón cavefish, *Astyanax mexicanus*. *Current Biology - CB*, 2021, 31 (21), pp.4800-4809.e9. 10.1016/j.cub.2021.08.030 . hal-03337251

**HAL Id: hal-03337251**

**<https://hal.inrae.fr/hal-03337251>**

Submitted on 14 Sep 2021

**HAL** is a multi-disciplinary open access archive for the deposit and dissemination of scientific research documents, whether they are published or not. The documents may come from teaching and research institutions in France or abroad, or from public or private research centers.

L’archive ouverte pluridisciplinaire **HAL**, est destinée au dépôt et à la diffusion de documents scientifiques de niveau recherche, publiés ou non, émanant des établissements d’enseignement et de recherche français ou étrangers, des laboratoires publics ou privés.



Distributed under a Creative Commons Attribution - NonCommercial - NoDerivatives 4.0 International License

1 **A supernumerary “B-sex” chromosome drives male sex**  
2 **determination in the Pachón cavefish, *Astyanax mexicanus***  
3

4 Boudjema Imarazene<sup>1,2</sup>, Kang Du<sup>3</sup>, Séverine Beille<sup>1</sup>, Elodie Jouano<sup>1</sup>, Romain Feron<sup>1,4,5</sup>,  
5 Qiaowei Pan<sup>1,4</sup>, Jorge Torres-Paz<sup>2</sup>, Céline Lopez-Roques<sup>6</sup>, Adrien Castinel<sup>6</sup>, Lisa Gil<sup>6</sup>, Claire  
6 Kuchly<sup>6</sup>, Cécile Donnadiou<sup>6</sup>, Hugues Parrinello<sup>7</sup>, Laurent Journot<sup>7</sup>, Cédric Cabau<sup>8</sup>, Margot  
7 Zahm<sup>9</sup>, Christophe Klopp<sup>9</sup>, Tomáš Pavlica<sup>10,11</sup>, Ahmed Al-Rikabi<sup>12</sup>, Thomas Liehr<sup>12</sup>, Sergey  
8 Simanovsky<sup>13</sup>, Joerg Bohlen<sup>10</sup>, Alexandr Sember<sup>10</sup>, Julie Perez<sup>14</sup>, Frédéric Veyrunes<sup>14</sup>, Thomas  
9 D. Mueller<sup>15</sup>, John H. Postlethwait<sup>16</sup>, Manfred Schartl<sup>3,17</sup>, Amaury Herpin<sup>1</sup>, Sylvie Rétaux<sup>2\*</sup>,  
10 Yann Guiguen<sup>1\*§</sup>  
11

12 **AUTHOR AFFILIATIONS**  
13

14 <sup>1</sup> INRAE, LPGP, 35000 Rennes, France.

15 <sup>2</sup> Université Paris-Saclay, CNRS, Institut des Neurosciences Paris-Saclay, 91198 Gif sur Yvette, France.

16 <sup>3</sup> Xiphophorus Genetic Stock Center, Department of Chemistry and Biochemistry, Texas State  
17 University, San Marcos, Texas, TX 78666, USA.

18 <sup>4</sup> Department of Ecology and Evolution, University of Lausanne, Lausanne, Switzerland.

19 <sup>5</sup> Swiss Institute of Bioinformatics, Lausanne, Switzerland.

20 <sup>6</sup> INRAE, GeT-PlaGe, Genotoul, 31326 Castanet-Tolosan, France.

21 <sup>7</sup> Institut de Génomique Fonctionnelle, IGF, CNRS, INSERM, Univ. Montpellier, F-34094 Montpellier,  
22 France.

23 <sup>8</sup> SIGENAE, GenPhySE, Université de Toulouse, INRAE, ENVT, Castanet Tolosan, France.

24 <sup>9</sup> SIGENAE, UMIAT, INRAE, Castanet Tolosan, France.

25 <sup>10</sup> Laboratory of Fish Genetics, Institute of Animal Physiology and Genetics, Czech Academy of  
26 Sciences, Rumburská 89, 27721 Liběchov, Czech Republic.

27 <sup>11</sup> Department of Zoology, Faculty of Science, Charles University, Viničná 7, 12844 Prague, Czech  
28 Republic.

29 <sup>12</sup> University Clinic Jena, Institute of Human Genetics, 07747 Jena, Germany.

30 <sup>13</sup> Severtsov Institute of Ecology and Evolution, Russian Academy of Sciences, Moscow, Russia.

31 <sup>14</sup> Institut des Sciences de l'Evolution de Montpellier (ISEM), CNRS, Université de Montpellier, IRD,  
32 34095 Montpellier, France.

33 <sup>15</sup> Department of Plant Physiology and Biophysics, Julius-von-Sachs Institute of the University  
34 Wuerzburg, D-97082 Wuerzburg, Germany.

35 <sup>16</sup> Institute of Neuroscience, University of Oregon, Eugene, USA.

36 <sup>17</sup> Department of Developmental Biochemistry, University of Wuerzburg, Wuerzburg, Germany.

37  
38 \* Equally contributing senior authors. § Lead contact: Yann Guiguen, INRAE, Laboratoire de  
39 Physiologie et Génomique des poissons, Campus de Beaulieu, 35042 Rennes cedex, France. Tel: +33  
40 2 99 46 58 09 ([yann.guiguen@inrae.fr](mailto:yann.guiguen@inrae.fr)). Twitter: @Houpss35

41  
42 **Key words:** Sex determination, cavefish, B chromosome, sex chromosomes, *gdf6*  
43

## 44 SUMMARY

45 Sex chromosomes are generally derived from a pair of classical type-A chromosomes, and  
46 relatively few alternative models have been proposed up to now<sup>1,2</sup>. B chromosomes (Bs) are  
47 supernumerary and dispensable chromosomes with non-Mendelian inheritance found in many  
48 plant and animal species<sup>3,4</sup>, that have often been considered as selfish genetic elements that  
49 behave as genome parasites<sup>5,6</sup>. The observation that in some species Bs can be either restricted  
50 or predominant in one sex<sup>7-14</sup> raised the interesting hypothesis that Bs could play a role in sex  
51 determination<sup>15</sup>. The characterization of putative B master sex-determining (MSD) genes,  
52 however, has not yet been provided to support this hypothesis. Here, in *Astyanax mexicanus*  
53 cavefish originating from Pachón cave, we show that Bs are strongly male-predominant. Based  
54 on a high-quality genome assembly of a B-carrying male, we characterized the Pachón cavefish  
55 B sequence and found that it contains two duplicated loci of the putative MSD gene growth  
56 differentiation factor 6b (*gdf6b*). Supporting its role as an MSD gene, we found that the Pachón  
57 cavefish *gdf6b* gene is expressed specifically in differentiating male gonads, and that its  
58 knockout induces male-to-female sex reversal in B-carrying males. This demonstrates that  
59 *gdf6b* is necessary for triggering male sex determination in Pachón cavefish. Altogether these  
60 results bring multiple and independent lines of evidence supporting the conclusion that the  
61 Pachón cavefish B is a “B-sex” chromosome that contains duplicated copies of the *gdf6b* gene  
62 which can promote male sex determination in this species.

63

## 64 RESULTS AND DISCUSSION

### 65 Pachón cavefish B chromosomes are male-predominant B chromosomes

66 Supernumerary B chromosomes (Bs) are generally thought to arise from the duplication and  
67 assembly of A chromosome sequences<sup>16-19</sup> and their relationship to sex chromosomes has often  
68 been suspected and discussed<sup>15</sup>. Some hypotheses state that Bs are derived from sex  
69 chromosomes or, alternatively, evolved to become sex chromosomes<sup>15,20-23</sup>. Because Bs have  
70 been described in *A. mexicanus*<sup>19,24,25</sup>, we performed cytogenetic analyses in 17 males and 11  
71 females of a laboratory population of Pachón cavefish (Pachón) to investigate whether Pachón  
72 Bs could be sex-restricted. We found that Pachón Bs are euchromatic mitotically unstable  
73 microchromosomes (Figure 1A-B, Figure S1), that are present in one to three copies in most  
74 male metaphases (mean number  $\pm$  SD of Bs per male metaphase =  $1.08 \pm 0.41$ ), contrasting  
75 with a barely detectable B occurrence in female metaphases (mean number  $\pm$  SD of Bs per  
76 female metaphase =  $0.05 \pm 0.08$ , Figure 1C and Data S1A). Chromosomal mapping by

77 fluorescence *in situ* hybridization (FISH) using probes generated from microdissected male Bs  
78 painted Bs in males and even the rare B in females, supporting that Pachón male-predominant  
79 Bs and the low occurrence female Bs share a similar gDNA content (Figure 1D). In addition,  
80 weaker FISH signals were also detected on different terminal parts of some A chromosomes  
81 (see small white arrows in Figure 1D), suggesting that Pachón Bs are made up of many  
82 duplicated fragments of A chromosomes<sup>16-19</sup>, and / or that they share repetitive DNAs with the  
83 A chromosomes<sup>21,24,26</sup>. Female or male sex-restricted or sex-predominant Bs have been  
84 described in many fishes, like for instance in some cichlids<sup>12-14</sup> and characiforms<sup>8,9,27,28</sup>. In *A.*  
85 *mexicanus*, Bs were recently described as being restricted only in some, but not all, males<sup>19</sup>,  
86 suggesting population differences in the frequency and sex-linkage of Bs that have also been  
87 reported in many species<sup>4-6,29</sup>. In addition to metaphase spreads (Figure 1E-F), we also detected  
88 Bs in pachytene chromosome spreads from testes of two Pachón males (N=52 and N=25).  
89 Single Bs were found in most cells (44/52 and 23/25) and always as unpaired chromosomes  
90 (Figure 1G-H). Hence, Pachón Bs are present in meiotic germ cells and they do not pair with  
91 A chromosomes in line with what has been found in other species with Bs<sup>30</sup>. The question of  
92 whether Pachón Bs can pair to each other remains open because we detected no case of multiple  
93 Bs in these pachytene chromosome spreads.

#### 94 **Characterization of the Pachón cavefish B chromosome sequence**

95 Because the publicly available Pachón genome assembly was obtained from a female<sup>31</sup>, we  
96 sequenced the genome of a B+ Pachón male to assemble its B sequence. Bs are notoriously  
97 difficult to assemble<sup>32,33</sup>, due to their complex mosaic composition of A chromosome  
98 fragments<sup>16-19</sup> and their high-repeat content<sup>17,19</sup>, and most of the B sequence information is  
99 from short-read sequencing of purified Bs<sup>17,18</sup> or B+ versus B-devoid (B-) individuals<sup>17-19,34</sup>.  
100 To accurately assemble a high-quality Pachón B sequence, we used a combination of HiFi  
101 PacBio and Oxford nanopore long-reads, 10X genomics Illumina short-linked reads, and a Hi-  
102 C chromosome contact map. The resulting whole-genome assembly (see assembly metrics in  
103 Data S1B) contains 25 large scaffolds corresponding to the 25 Pachón A-chromosome pairs<sup>19,25</sup>  
104 and 170 remaining unplaced scaffolds (2.12% of the total assembly size).

105 To identify the Pachón B sequence we used its male-predominant feature and a pool-  
106 sequencing (pool-seq) approach to contrast whole-genome sequences of a genomic DNA  
107 (gDNA) pool of 91 phenotypic males versus a gDNA pool of 81 phenotypic females. By  
108 remapping these male and female pool-seq reads on our male Pachón genome assembly, we

109 identified a single 2.97 Mb unplaced scaffold (HiC\_Scaffold\_28) that displays a clear male-  
110 biased read coverage profile (Figure 2A-A'). The sequence analysis of HiC\_Scaffold\_28  
111 revealed that it is made up from a complex mosaic of numerous duplicated fragments of A  
112 chromosomes (Figure 2B) including complete but also truncated duplicates of A chromosome  
113 genes (Table S3). The B also displays a repeat content that is markedly different from A  
114 chromosomes (Figure 2C-D, Figures S2A-B, Data S1D). Both its sex-biased profile and its  
115 sequence characteristics indicate that HiC\_Scaffold\_28 is the Pachón B. The contribution of  
116 many A chromosome regions to the structure of Pachón Bs is in line with the recent findings  
117 that *A. mexicanus* Bs contain a large number of transposable elements<sup>19</sup>. The high B proportion  
118 of satellite DNA (Figures S2 and Data S1D), was also reported in other species<sup>35</sup>. Our  
119 manually curated B gene annotation (Data S1C) identified 63 genes on the Pachón B. Of these,  
120 20 show high-quality annotation over their full length, 11 are truncated compared to their  
121 conserved homologs in other fish and one is a chimeric gene. Five genes show multiple copies  
122 and constitute almost one-third of the B gene content (Data S1C). These results contrast with  
123 earlier studies which reported a much higher number of B genes in *A. mexicanus*<sup>19</sup>. These  
124 annotation differences are likely due to indirect assessment of the B gene content based on  
125 short-read sequencing of very few B+ versus B- individuals<sup>19</sup>. This comparison clearly  
126 illustrates the need for better, complete and high-quality B assemblies like we provided here  
127 for Pachón cavefish, to better understand the structure and gene content of Bs generally.

### 128 **The Pachón cavefish B contains two copies of a putative master sex determining gene**

129 Among the B genes with well-supported annotation evidence (Data S1C), we identified two  
130 duplicated loci of the A-chromosome-3 growth differentiation factor 6b (*gdf6b*) gene (located  
131 at Chr03:863,919-866,170), that is the teleost ohnolog (teleost whole genome duplication<sup>36,37</sup>  
132 paralogous copy) of the *gdf6a* gene (Figure 3A). *Gdf6* genes belong to the TGF- $\beta$  superfamily  
133 within which many master sex-determining (MSD) genes have been found, including TGF- $\beta$   
134 receptors<sup>38-40</sup> and ligands<sup>41-44</sup>. Of note, *gdf6a* on the Y chromosome (*gdf6aY*) has been  
135 characterized as the master sex-determining gene in the turquoise killifish, *Nothobranchius*  
136 *furzeri*<sup>44</sup>. The Pachón B *gdf6b* genes (*B-gdf6b* = *B-gdf6b-1* and *B-gdf6b-2*) were thus retained  
137 as potential candidate B MSD genes. Chromosome FISH hybridization with a *gdf6b* locus  
138 probe revealed a *gdf6b* hybridization signal on the Pachón Bs, along with a single *gdf6b*  
139 labelling on a single A chromosome pair, both in the male-predominant Bs and the low  
140 occurrence female Bs (Figure 1E-F, and inset in Figure 1E).

141 The two *B-gdf6b* loci are 99.6 % identical in the 21.6 kb region shared by the two genes, and  
142 100% identical in their coding sequences (CDS), with *B-gdf6b-2* being derived from an internal  
143 B duplication of the *B-gdf6b-1* locus (Figure S2C). Such internal B duplications / insertions  
144 indicate that the origin of the B structure can be more complex than initially thought.  
145 Comparison of these *B-gdf6b* loci with the overlapping sequence of their A chromosome  
146 counterpart (*A-gdf6b*) revealed numerous differences in their proximal promoters and also their  
147 intron that contains two *B-gdf6b* specific insertions (Figure S2D). However, differences within  
148 the *gdf6b* CDS were limited to a T-to-C (*A-gdf6b*-to-*B-gdf6b*) synonymous substitution  
149 (c.591T>C) and two nonsynonymous substitutions, i.e., a T-to-G (*A-gdf6b*-to-*B-gdf6b*)  
150 transversion (c.180T>G) in exon 1 that switches a A-Gdf6b lysine into a B-Gdf6b asparagine  
151 (p.Lys60Asn) and a G-to-A (*A-gdf6b*-to-*B-gdf6b*) transition (c.679G>A) in exon 2 that  
152 switches the A-Gdf6b serine into a B-Gdf6b glycine (p.Ser227Gly) (Figure S2E). The  
153 Lys60Asn does not impact a conserved amino-acid position of Gdf6b proteins, in contrast to  
154 the Ser227Gly that impacts a glycine of the TGF- $\beta$ /BMP propeptide domain that is conserved  
155 in Pachón B-Gdf6b and in all vertebrate Gdf6 proteins, but not in Pachón A-Gdf6b (Figure  
156 3B). It is interesting to note that this Ser227Gly modification suggests that the *A-gdf6b* acquired  
157 this mutation after the *B-gdf6b* copy was duplicated on the B chromosome. This non-conserved  
158 Ser227 engages in a central hydrogen bond network at a looptip region in the TGF- $\beta$ /BMP  
159 propeptide domain (Figure 3C) that could affect the stability of this pro-domain. The  
160 Gly227Ser exchange in Pachón A-Gdf6b leads to the gain of several hydrogen bonds that are  
161 due to the side chain hydroxyl group of the Ser227 residue (Figure 3D-E). The gain of hydrogen  
162 bonds can confer a higher folding stability of the proprotein complex and thereby might affect  
163 activation of Gdf6b as this requires release of the mature C-terminal domain from the  
164 proprotein complex. The mature C-terminal growth factor domain, however, is likely to be  
165 unaffected by this mutation. Whether these conformation differences between the A-Gdf6b and  
166 B-Gdf6b proproteins could provide a potential functional explanation for a sex-determining  
167 role of the male-predominant Pachón B-Gdf6b remains to be explored, but point mutations in  
168 other MSD genes like *amhr2Y* in *Takifugu rubripes* and *amhY* in *Oreochromis niloticus*, have  
169 been described to be directly responsible for male sex determination<sup>39,41</sup>.

170 Based on these *B-gdf6b* and *A-gdf6b* loci differences, we developed several B-specific PCR  
171 genotyping tests on fin clips (Figure S3A). In our Pachón laboratory population, we found a  
172 complete (100%) association between B-specific amplifications and the male phenotype in 723  
173 males, with all the 787 tested females being negative (p-value of association with sex < 2.2e-

174 16). We also found the same complete association in wild-caught Pachón individuals (20 males  
175 and 20 females, recognized by external sex-specific traits without sacrifice; p-value of  
176 association with sex = 1.87e-09) (Data S1F) showing that this male-predominant B is not the  
177 result of a domestication effect. These results strengthen our cytological observations of a male-  
178 predominant B. The absence of B-specific amplifications in females despite the cytogenetic  
179 detection of rare Bs in females is probably the result of a PCR sensitivity issue as increasing  
180 the number of PCR cycles allows the detection of a faint PCR fragment in Pachón females  
181 (Figure S3B).

## 182 **Evidence supporting *gdf6b* as a potential master sex determining gene in Pachón cavefish**

183 Sex-specific expression patterns during the sex differentiation period and alteration of gonadal  
184 development upon knockout are key arguments for the evaluation of a candidate MSD gene.  
185 Due to the high sequence identity of the *B-gdf6b* and *A-gdf6b* cDNAs, we were not able to  
186 specifically quantify the *B-gdf6b* expression. Quantification of the expression of *gdf6b* (*B-*  
187 *gdf6b* and/or *A-gdf6b*) showed that it has both a predominant expression in developing and  
188 adult male gonads (as well as in male brain, intestine, kidney and swim-bladder; Figure S4A)  
189 and a strong sexually dimorphic expression during early differentiation of B+ individuals  
190 (Figure 4A). Using *in situ* hybridization, the expression of *gdf6b* during the early differentiating  
191 period was restricted to gonads of B+ individuals (at 15, 21, 30, and 60 days post-fertilization),  
192 with no strict colocalization with the gonadal soma-derived factor gene (*gsdf*) (Figure 4B-C  
193 and Figure S4B). *Gsdf* is a well-known gonad-restricted, somatic supporting cell lineage  
194 marker<sup>45-47</sup> that has also been described as one of the earliest Pachón gonadal sex  
195 differentiation marker genes<sup>48</sup>. This result demonstrates that *gdf6b* mRNA (*B-gdf6b* and/or *A-*  
196 *gdf6b*) has an expression profile compatible with a male (B+) MSD function, being expressed  
197 in the right place, i.e., only in the differentiating testis, and at the right time, i.e., during early  
198 testicular differentiation.

199 To bring additional and functional evidence that *gdf6b* could act as an MSD gene, we generated  
200 *gdf6b* knockouts in Pachón cavefish using the genome-editing CRISPR-Cas9 system with two  
201 guide RNAs in order to remove a large part of the *gdf6b* CDS (Figure 4D). This large deletion  
202 (~470 bp) includes most of the TGF- $\beta$  propeptide region and the beginning of the TGF- $\beta$  like  
203 domain resulting in a truncated, likely non-functional, Gdf6b protein (Figure S2F). Among 200  
204 first-generation microinjected individuals (which are mosaic for the genome-edited loci),  
205 eighteen B+ individuals (i.e., genotypic males) had a ~470 bp deletion in their *A-* and/or *B-*

206 *gdf6b* exon 2 (Figure S3C), and they were all sex-reversed into phenotypic females (Figure  
207 4G). In contrast, all B+ males and B- females without the *gdf6b* deletion developed normal  
208 testes (B+) or ovaries (B-) (Figure 4E-F). This result shows that *gdf6b* is necessary to trigger  
209 Pachón testicular development in B+ individuals and brings further functional evidence that  
210 *gdf6b* could be used as a male MSD gene in Pachón cavefish. However, because of the high  
211 similarity of the *B-gdf6b* loci with the *A-gdf6b* locus, we have not been able to specifically  
212 knockout the Pachón *B-gdf6b*. Further studies will bring more functional proof supporting the  
213 role of the *B-gdf6b* genes in sex determination, including the specific *B-gdf6b* knockout in B+  
214 individuals and the overexpression of *gdf6b* by transgenesis in B- fish.

## 215 **Conclusions**

216 Altogether our results bring new pieces of evidence to support a role of some B chromosomes  
217 in sex determination. The potential implication of Bs in sex determination had been suspected  
218 in many species including some fishes<sup>14,15</sup>. Up to now, however, the characterization of  
219 potential B MSD genes along with strong functional evidence has only been provided for the  
220 bacterial-derived *haploidizer* gene in the jewel wasp, *Nasonia vitripennis* B chromosome  
221 (named PSR for paternal sex ratio chromosome)<sup>49</sup>, although maleness in this haplo-diploid  
222 organism is determined through elimination of the paternal A chromosome set<sup>50</sup>. Here,  
223 combining a variety of approaches we discovered that Pachón cavefish of the species *A.*  
224 *mexicanus* carry male-predominant Bs that contain two copies of the *gdf6b* gene, which itself  
225 behaves as an excellent MSD candidate gene. This indeed brings the interesting hypothesis that  
226 these Pachón Bs could be considered as “B-sex” chromosomes. However, the question remains  
227 open whether Pachón Bs are predominant in males because they are eliminated from female  
228 tissues or whether they are by themselves necessary and sufficient to trigger maleness. Despite  
229 being male-predominant, Pachón Bs are also found in some females albeit only in very few  
230 metaphases (21.6 times less abundant than in males on average) and most often as a single B  
231 copy. B frequencies have been described as being highly variable between species, sexes,  
232 individuals of the same population, and even in different cells of a single individual<sup>4-6,29</sup>. This  
233 variation is assumed to result from meiotic and/or mitotic instability of Bs that can be present  
234 only in some organs and absent from others<sup>4,29,51-53</sup>. In the plant *Aegilops speltoides*, a  
235 mechanism of programmed elimination of Bs occurs specifically in the roots<sup>54</sup>. It results from  
236 a B chromatid nondisjunction during mitosis, leading to the micronucleation of Bs and their  
237 subsequent degradation at early stages of the proto-root embryonic tissue differentiation<sup>54</sup>.  
238 Such a mechanism would potentially explain a specific B elimination in Pachón female organs,



239 as it has been hypothesized in another *Astyanax* species with male-restricted Bs<sup>11</sup>. Further  
240 studies are now needed to better understand this sex-specific B drive mechanism, and if it  
241 reflects a cause or a consequence of sex determination in Pachón cavefish. Our results also lay  
242 a high-quality genome-based foundation in an important emerging fish model for studying the  
243 genomic evolution of Bs, including the micro- and macro-evolution of this B chromosome in  
244 line with the evolution of sex chromosomes.

245

## 246 **ACKNOWLEDGEMENTS**

247 We thank Victor Simon, Stéphane Père, Krystel Saroul, Pierre-Lo Sudan and Amélie Patinote  
248 for taking care and handling cavefish, and Manon Thomas and the LPGP TEFOR infrastructure  
249 platform for acquisition of the RNAScope confocal images. This project was supported by  
250 funds from the “Agence Nationale de la Recherche” (ANR/DFG, PhyloSex project, 2014-  
251 2016) to Y.G and M.S. S.R was supported by grants from an Equipe FRM (Fondation pour la  
252 Recherche Médicale, DEQ20150331745) and MITI CNRS (Mission pour les Initiatives  
253 Transverses et Interdisciplinaires). J.H.P was supported by a NIH grant (R35 GM139635).  
254 Sequencing was supported by France Génomique as part of an “Investissement d’avenir”  
255 program managed by ANR (contract ANR-10-INBS-09) and by the GET-PACBIO program («  
256 Programme opérationnel FEDER-FSE MIDI-PYRENEES ET GARONNE 2014-2020 »). The  
257 CytoEvol platform at ISEM was supported by the Labex CeMEB. J.B, T.P and A.S were  
258 supported by RVO: 67985904 of IAPG CAS, Liběchov. T.P was supported by the projects of  
259 the Czech Ministry of Education (SVV 260571/2021). S.S was supported by the Russian  
260 Foundation for Basic Research (RFBR) (18-34-00638). B.I PhD fellowship was supported by  
261 the Doctoral School of Ecology, Geosciences, Agronomy, Nutrition of the University of  
262 Rennes 1 and INRAE. We are grateful to the genotoul bioinformatics platform Toulouse  
263 Occitanie (Bioinfo Genotoul, <https://doi.org/10.15454/1.5572369328961167E12>) for  
264 providing help, computing and storage resources. Funders had no role in study design, data  
265 collection and analysis, decision to publish, or preparation of the manuscript.

266

## 267 **AUTHOR CONTRIBUTIONS**

268 Conceptualization, S.R., A.H. and Y.G.; Methodology, B.I., S.R., A.H., A.S., and Y.G.; Formal  
269 Analysis, T.D.M., K.D., R.F., Q.P., C.C., M.Z., and C.K.; Investigation, B.I., S.B., E.J., J.T-P.,

270 C.L-R., A.C., L.G., C.K., C.D., H.P., L.J., T.P., A.A-R., T.L., S.S., J.B., A.S., J.P., F.V.;

271 Writing –Original Draft, B.I., S.R., and Y.G.; Writing –Review & Editing, A.S., J.H.P.,

272 T.D.M., and M.S.; Visualization, B.I., K.D., E.J., R.F., Q.P., C.C., A.S., T.D.M., and Y.G.;

273 Funding Acquisition, S.R., M.S., J.H.P., and Y.G.; Supervision, S.R., A.H., and Y.G.

274

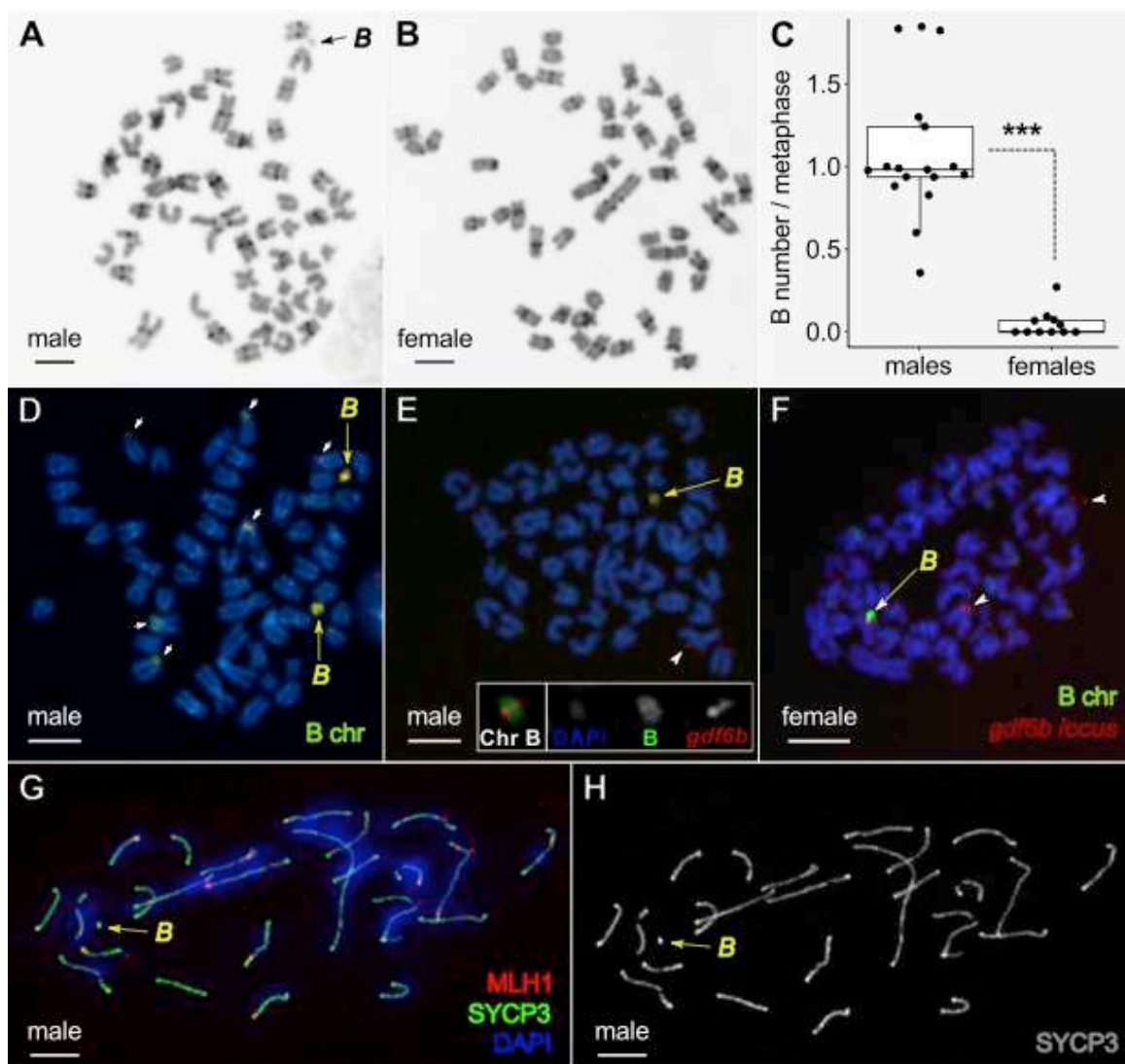
275 **DECLARATION OF INTERESTS**

276 The authors declare no competing interests

277

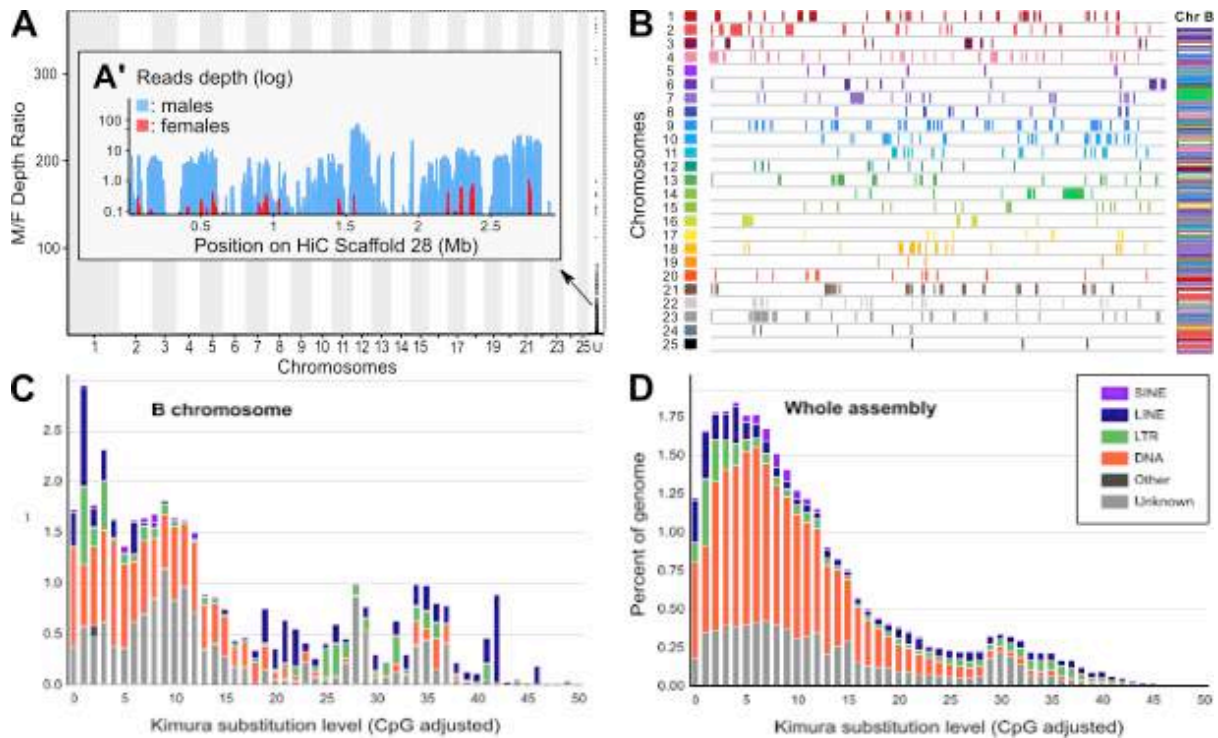
278 **FIGURE**

279



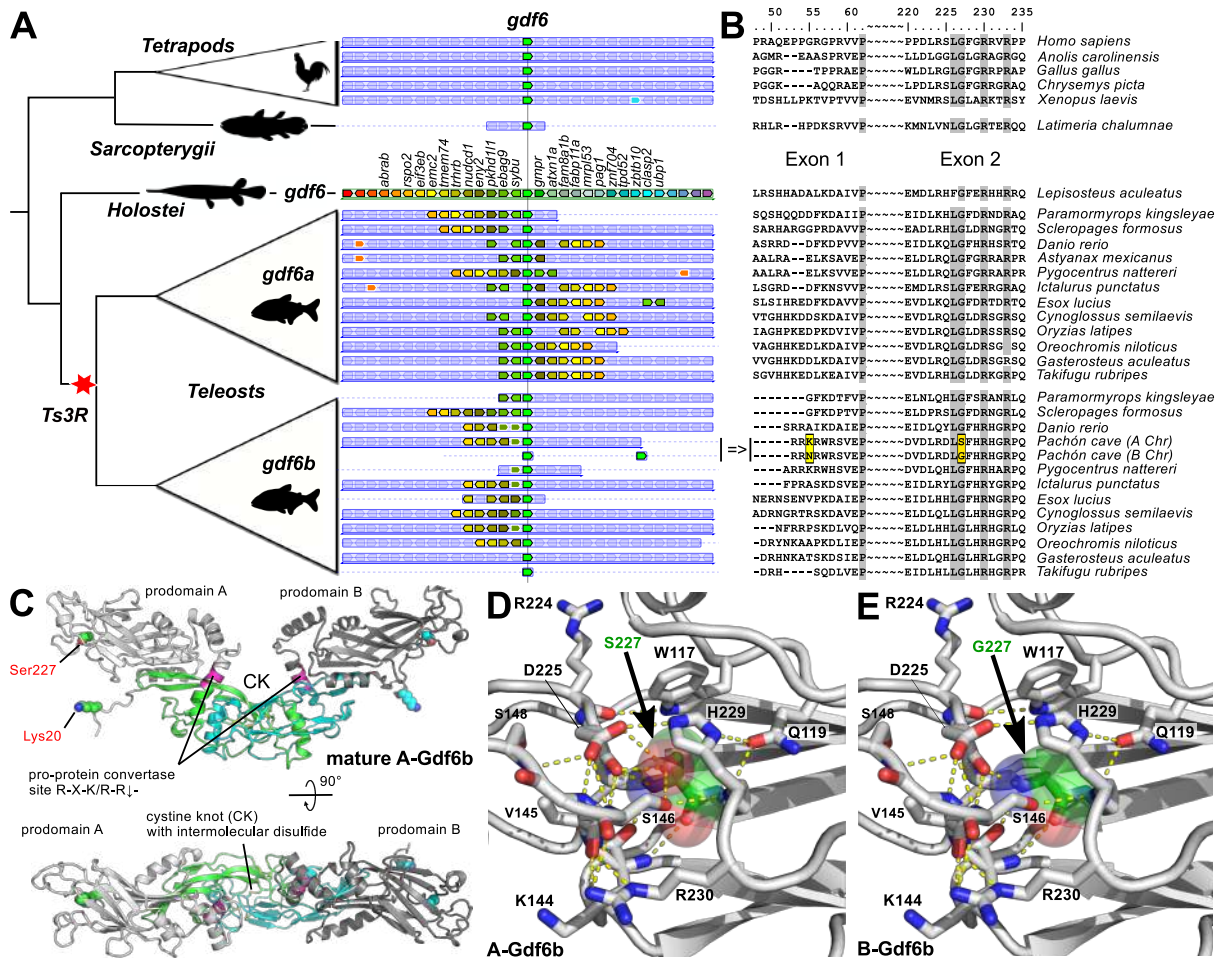
280

281 **Figure 1: Karyological characterization of male-predominant supernumerary B**  
282 **chromosomes (Bs) in Pachón cave *Astyanax mexicanus*. A-B:** Representative C-banding  
283 patterns of single B+ male (**A**) and B- female (**B**) from Pachón cave. The Bs (black arrow) lack  
284 C-bands, suggesting that Pachón cavefish Bs are largely euchromatic. See also Figure S1. **C:**  
285 Boxplots of the average number of Bs per metaphase in Pachón cavefish males and females.  
286 Horizontal lines indicate the median, the box indicates the interquartile range (IQR), and the  
287 whiskers the range of values that are within 1.5 x IQR. Statistical significance between males  
288 and females were tested with the Wilcoxon Rank Test (\*\*\*) =  $P < 0.001$ ). See also Data S1A.  
289 **D:** Fluorescence *in situ* hybridization (FISH) of male Pachón cave mitotic metaphase labeled  
290 with combined microdissected B probes. Yellow arrows point to the strong labelling of Bs and  
291 the small white arrows to the lighter labelling of some different parts of A chromosomes. **E-F:**  
292 FISH co-labelling of a 1B male (**E**) and a 1B female (**F**) metaphase with microdissected B  
293 (green) and *gdf6b*-specific (red) probes. Bs are indicated by yellow arrows and the white  
294 arrowheads point to pairs of A chromosome sister chromatids labelled by the *gdf6b* probe. Only  
295 one A-chromosome *gdf6b* signal was detected in panel **E**. The two *gdf6b* signals (see inset in  
296 **E**) that were often visible on male metaphases, cannot be interpreted as the two different B-  
297 *gdf6b* loci due to their genomic proximity (see Table S3) and the FISH resolution. **G-H:**  
298 Synaptonemal complex (SC) analysis showing that Pachón cave Bs (yellow arrow) do not pair  
299 with the 25 fully synapsed standard bivalents of A chromosomes. SCs were visualized by anti-  
300 SYCP3 antibody (green), the recombination sites were identified by anti-MLH1 antibody (red)  
301 and chromosomes were counterstained by DAPI (blue). **G:** Merged image. **H:** SYCP3  
302 visualization only. Scale bars = 5  $\mu\text{m}$ .



303

304 **Figure 2: Genomic characterization of Pachón cavefish B chromosome (B).** **A:** Read depth  
 305 ratio of male and female Pachón genomic pools showing a strong coverage bias in a single  
 306 scaffold, Hi\_scaffold\_28 (enlarged in **A'** inset showing male and female read coverage). **B:**  
 307 Karyoplots of the A chromosome regions duplicated on the Pachón cavefish B (Chr B) showing  
 308 that the Pachón B is made from a complex mosaic of duplicated A chromosomal fragments. **C-**  
 309 **D:** Comparison of the repeat landscapes of the Pachón B (**C**) and whole-genome including the  
 310 B (**D**), showing that the Pachón B has a very different repeat element (color code provided in  
 311 inset of panel C) content compared to A chromosomes. Short interspersed repeated sequences  
 312 (SINEs), long interspersed nuclear elements (LINEs), long terminal repeats (LTRs), DNA  
 313 repeat elements (DNAs), and terminal inverted repeat sequences (TIRs). See also Figure S2A-  
 314 B and Data S1D for additional details.

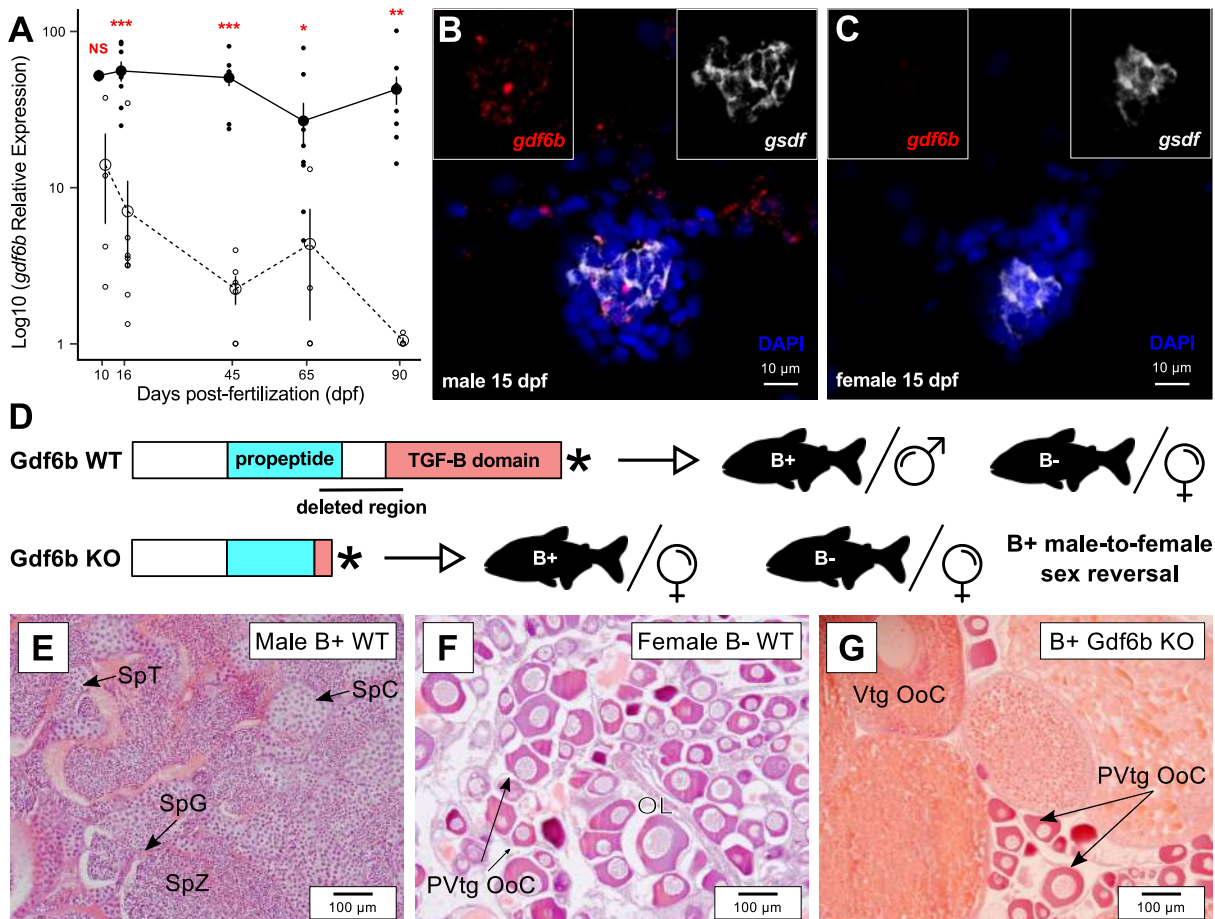


315

316 **Figure 3: Gdf6b protein evolution and structure.** **A:** Simplified phylogeny (left panel) and  
 317 synteny (middle panel) relationships of the *gdf6a* and *gdf6b* genes, with the additional *B-gdf6b*  
 318 Pachón cavefish duplication, showing that they are duplicated paralogues stemming from the  
 319 teleost whole genome duplication (Ts3R). Species names are given on the right side of panel  
 320 B. **B:** Corresponding multiple alignments of Gdf6 protein-coding sequences around the A-  
 321 Gdf6b lysine to B-Gdf6b asparagine switch in Exon 1 (p.Lys60Asn) and the A-Gdf6b serine  
 322 to B-Gdf6b glycine switch in Exon 2 (p.Ser227Gly). **C:** Ribbon plot homology model of A-  
 323 Gdf6b proprotein dimer (bottom panel view is rotated by 90° around the x-axis). The  
 324 prodomains are shown in light and dark grey, the furin processing site (R274-R-K-R-R278) is  
 325 indicated in magenta, the activity-containing mature C-terminal domain is shown in green and  
 326 cyan. The two residues differing between A-Gdf6b and B-Gdf6b are presented as spheres with  
 327 their carbon atoms colored in green and cyan. **D-E:** Comparative magnifications of the  
 328 structure of A-Gdf6b (**D**) and B-Gdf6b (**E**) around the p.Ser227Gly switch. Amino acid  
 329 residues interacting with Ser227 or Gly227 are shown as sticks, and hydrogen bonds are shown  
 330 as yellow stippled lines. As shown, the side chain hydroxyl group of Ser227 (shown with carbon atoms  
 331 colored in green and transparent spheres highlighting the van der Waals spheres of the atoms)



332 engages in several hydrogen bonds with surrounding residues, e.g. Ser146, Asp225 thereby  
 333 stabilizing the tertiary and secondary structure in this region. Upon exchange of Ser227 with a  
 334 glycine as in B-Gdf6b these hydrogen bonds are lost thereby potentially destabilizing this  
 335 region in the prodomain.



336

337 **Figure 4: Gene expression and functional evidence supporting a role of *gdf6b* as a**  
 338 **potential master sex-determining gene in Pachón cavefish. A:** Expression profiles of *gdf6b*  
 339 in male and female trunks during early development from 10 to 90 days post-fertilization (dpf,  
 340 males: solid line; females: dashed line) showing a significant over-expression in males  
 341 compared to females starting from 16 dpf. Results are presented as log<sub>10</sub> mean ± standard  
 342 errors; black and white dots represent the individual values of relative expression in males and  
 343 females, respectively. Statistical significance between males and females was tested with the  
 344 Wilcoxon Rank Sum Test (Wilcoxon-Mann-Whitney Test) and only significant differences are  
 345 shown (\*\*\* = P < 0.01; \*\* = P < 0.01; \* = P < 0.05). **B-C:** Gonadal expression of *gdf6b* (in  
 346 red) and the Sertoli and granulosa supporting cell marker *gsdf* (in white) in male (**B**) and female  
 347 (**C**) differentiating gonads at 15 dpf showing that *gdf6b* is specifically expressed in male gonads  
 348 with no strict colocalization with *gsdf* in male. See Figure S6B for additional stages of

349 development. Nuclei were stained with DAPI (in blue). Scale bar = 10  $\mu$ m. **D:** Schematic  
350 representation of the wild-type (WT) and knock-out (KO) *Gdf6b* proteins and the resulting  
351 phenotypes of B+ males and B- females. **E-F:** Representative gonadal histology of WT males  
352 (**E**), WT females (**F**), and *Gdf6b KO* B+ males showing that *Gdf6b KO* induces male-to-female  
353 sex reversal (**G**) with ovaries containing vitellogenic (Vtg Ooc) and previtellogenic oocytes  
354 (PVtg Ooc), like WT ovaries (**F**), contrasting with the testis in WT males (**E**). Ol: Ovarian  
355 lamellae. SpC: Spermatocytes; SpG; Spermatogonia; SpT: Spermatids; SpZ: Spermatozoa.  
356 Scale bar = 100  $\mu$ m. See also Figure S4.

## 357 358 **STAR METHODS**

359

## 360 **RESOURCE AVAILABILITY**

### 361 **Lead contact**

362 Further information and requests for resources and reagents should be directed to and will be  
363 fulfilled by the lead contact, Yann Guiguen (yann.guiguen@inrae.fr).

364

### 365 **Materials availability**

366 To request Pachón fish lines or constructs created in this study, please contact the lead contact.

367

### 368 **Data and code availability**

369 Raw sequences and the whole genome assembly of Pachón cavefish have been deposited in the  
370 National Center for Biotechnology Information DDBJ/ENA/GenBank databases under the  
371 BioProject PRJNA734455. This accession number is listed in the key resources table. This  
372 study did not generate new unique code. Any additional information required to reanalyze the  
373 data reported in this paper is available from the lead contact upon request.

374

375

## 376 **EXPERIMENTAL MODEL AND SUBJECT DETAILS**

### 377 ***Cavefish breeding and sampling***

378 Laboratory stocks of *A. mexicanus* Pachón cavefish were obtained in 2004 from the Jeffery  
379 laboratory at the University of Maryland, College Park, MD. Fish were raised as previously  
380 described. Fertilized eggs were provided by CNRS cavefish experimental facilities (Gif sur  
381 Yvette, France) and maintained at 24°C until the hatching stage occurring around 24  $\pm$  2 hours

382 post-fertilization (hpf)<sup>55</sup>. Subsequently, larvae were transferred and raised in the Fish  
383 Physiology and Genomics laboratory experimental facilities (LPGP, INRAE, Rennes, France)  
384 under standard photoperiod (12 h light / 12 h dark) and at two different temperatures:  $21 \pm 1$   
385 °C and  $28 \pm 1$ °C. Animals were fed twice a day, firstly with live artemia (Ocean Nutrition)  
386 until 15 days post-fertilization (dpf), then with a commercial diet (BioMar) until adult stage.  
387 For animal dissections and organ sampling, fish were euthanized with a lethal dose of tricaine  
388 methanesulfonate (MS 222, 400 mg/l), supplemented by 150 mg/l of sodium bicarbonate.  
389 Phenotypic sex of individuals was determined at 4 months and more, either by macroscopical  
390 examination of the gonads when they were enough differentiated, or by histology when gonads  
391 were not totally differentiated<sup>48</sup>. Caudal fin clips were collected from all individuals and stored  
392 in ethanol 90% at 4°C before genomic DNA (gDNA) extraction. For the chromosome contact  
393 map (Hi-C), 80 µl of blood was sampled from three males using a syringe rinsed with EDTA  
394 2%. The fresh blood was slowly frozen in a Freezing Container (Mr. Frosty, Nalgene®) after  
395 addition of 15% of dimethyl sulfoxide (DMSO). Karyotypic analyses were carried out in 17  
396 males and 11 females of Pachón cave *Astyanax mexicanus*. Fin samples (a narrow strip of the  
397 tail fin) were taken from the live specimens anesthetized by MS-222 (Merck KGaA, Darmstadt,  
398 Germany), while for direct preparations (chromosomes from kidneys and gonads), fishes were  
399 euthanized first using 2-phenoxyethanol (Sigma-Aldrich, St. Louis, MO, USA).

400 All animal protocols were carried out in strict accordance with the French and European  
401 legislations (French decree 2013-118 and directive 2010-63-UE) applied for ethical use and  
402 care of laboratory animals used for scientific purposes. Sylvie Retaux and CNRS institutional  
403 authorizations for maintaining and handling *A. mexicanus* in experimental procedures were 91-  
404 116 and 91272105, respectively. For karyotypic analysis, all handling of fish individuals  
405 followed European standards in agreement with §17 of the Act No. 246/1992 to prevent fish  
406 suffering. The procedures involving fish were supervised by the Institutional Animal Care and  
407 Use Committee of the Institute of Animal Physiology and Genetics CAS, v.v.i., the  
408 supervisor's permit number CZ 02361 certified and issued by the Ministry of Agriculture of  
409 the Czech Republic. Several sampling campaigns were carried out in the field in Mexico  
410 between 2013 and 2019, resulting in a collection of tail fin clips from wild-caught individuals  
411 from the Pachón cave. In the field, the phenotypic sex of animals was determined by checking  
412 the presence or absence of denticles on the anal fins as described previously<sup>56</sup>, a small fin clip  
413 was gently taken and fish were rapidly returned to their natural pond. In addition, pictures of  
414 each individual sampled were taken to confirm the phenotypic sex, back in the laboratory,



415 based on the morphological criteria described previously<sup>56</sup>. The permits for field sampling  
416 (02241/13, 02438/16, 05389/17 and 1893/19) were delivered by the Mexican authorities  
417 (Mexican Secretaría del Medio Ambiente y Recursos Naturales) to Sylvie Rétaux and  
418 Patricia Ornelas-Garcia (UNAM, Mexico).

419

## 420 **METHOD DETAILS**

### 421 ***DNA extraction***

422 For fish genotyping, gDNA was extracted from fin clips stored in 90% ethanol, after lysis in  
423 5% chelex<sup>57</sup> and 10 mg Proteinase K at 55 °C for 2 h, followed by 10 min at 99 °C. Following  
424 extraction, samples were centrifuged and the supernatant containing the gDNA was transferred  
425 in clean tubes and stored at -20 °C. For pool-sequencing and TaqMan assay, gDNA was  
426 extracted using NucleoSpin Kits for Tissue (Macherey-Nagel, Duren, Germany) according to  
427 the supplier's recommendations. For long-read male genome sequencing, high molecular  
428 weight (HMW) gDNA was extracted from a mature testis grounded in liquid nitrogen and lysed  
429 in TNES-Urea buffer (TNES-Urea: 4M urea; 10 mM Tris-HCl, pH 7.5; 120 mM NaCl; 10 mM  
430 EDTA; 5% SDS) for two weeks at room temperature. For HMW gDNA extraction the TNES-  
431 Urea solution was supplemented with Proteinase K at a final concentration of 150 µg/ml and  
432 incubated at 37 °C overnight. HMW gDNA was extracted with a modified phenol-chloroform  
433 protocol as previously described<sup>43</sup>. The gDNA concentrations for both pool-seq and genome  
434 sequencing were quantified with Qubit3 fluorometer (Invitrogen, Carlsbad, CA) and HMW  
435 gDNA quality and purity were assessed using spectrophotometry, fluorometry, and capillary  
436 electrophoresis.

### 437 ***Primers and probe design***

438 All primers used in this study including PCR genotyping, qPCR gene expression and cDNA  
439 cloning were designed using Primer3web software<sup>58</sup> version 4.1.0 and are listed in Data S1E.

### 440 ***B polymerase chain reaction (PCR) genotyping***

441 Genetic sex of Pachón cave individuals was determined by PCR tests using the fact that males  
442 have a B-predominant chromosome with three different sets of primers (see Table S6 for primer  
443 sequences) based on differences between the *A-gdf6b* and *B-gdf6b* loci. Three sets of primers  
444 (P) were designed (see Figure S3A) with two primer sets designed to amplify specifically the

445 two *B-gdf6b* copies based either on a single base variation between the A/B *gdf6b* CDS at  
446 position 679 bp (P1-P2), or based on primers located on both sides of the A/B breakpoints  
447 downstream of the *B-gdf6b* gene (P3-P4). The third set of primers (P5-P6) was designed on  
448 gaps/indels variations between *A-gdf6b* and the two *B-gdf6b* genes in the proximal promoter  
449 of *gdf6b* genes. Another set of primers (P9-P10) was designed as a PCR positive control with  
450 primers located on both sides of the A/B breakpoints downstream of the *A-gdf6b* gene. Primer  
451 sets P1-P2 and P3-P4 produce a single PCR fragment only in males (B+), primer set P5-P6  
452 amplifies two bands in males (all B+) and only a single band in females (all B-), and primer set  
453 P9-P10 amplifies a single band in all individuals. For PCR reactions with the P1-P2 primer set,  
454 HiDi Taq DNA polymerase (myPOLS Biotec) was used for detecting a single nucleotide  
455 variation. PCRs were performed in a total volume of 12.5  $\mu$ l containing 0.2  $\mu$ M of each primer,  
456 a final concentration of 20 ng/ $\mu$ l gDNA, 200  $\mu$ M of dNTPs mix, 1X of HiDi buffer (10X), and  
457 2.5 U per reaction of HiDi DNA polymerase. Cycling conditions were as follows: 95  $^{\circ}$ C for 2  
458 min, then 35 cycles of (95  $^{\circ}$ C for 15 seconds (secs) + 60  $^{\circ}$ C for 10 sec + 72  $^{\circ}$ C for 30 sec), and  
459 72  $^{\circ}$ C for 5 min. For PCR reactions with the P3-P4 and P9-P10 primer sets, PCR reactions were  
460 performed in a final volume of 50  $\mu$ l containing 0.5  $\mu$ M of each primer, a final concentration  
461 of 20 ng/ $\mu$ l gDNA, 10  $\mu$ M dNTPs mix, 1X of 10X AccuPrime<sup>TM</sup> buffer, and 0.5  $\mu$ l per reaction  
462 of AccuPrime<sup>TM</sup> Taq DNA polymerase. Cycling conditions were as follows: 94  $^{\circ}$ C for 2 min,  
463 then 35 cycles of (94  $^{\circ}$ C for 30 sec + 58  $^{\circ}$ C for 30 sec + 68  $^{\circ}$ C for 1 min and 30 sec). For PCR  
464 reactions with the P5-P6 primer set, PCR reactions were performed in a final volume of 25  $\mu$ l  
465 containing 0.5  $\mu$ M of each primer, a final concentration of 20 ng/ $\mu$ l gDNA, 10  $\mu$ M dNTPs  
466 mixture, 1X of Jumpstart<sup>TM</sup> buffer (10X), and 0.5  $\mu$ l per reaction of Jumpstart<sup>TM</sup> Taq DNA  
467 polymerase. Cycling conditions were as follows: 95  $^{\circ}$ C for 2 min, then 35 cycles of (95  $^{\circ}$ C for  
468 1 min + 60  $^{\circ}$ C for 30 sec + 72  $^{\circ}$ C for 1 min), and 72  $^{\circ}$ C for 5 min.

#### 469 **10 $\times$ Genomics sequencing**

470 10X Chromium Library was prepared according to 10X Genomics protocols using the Genome  
471 Reagent Kits v2. Optimal performance has been characterized on input gDNA with a mean  
472 length greater than 50 kb (~144Kb). GEM reactions were performed on 0.625 ng of genomic  
473 DNA, and DNA molecules were partitioned and amplified into droplets to introduce 16-bp  
474 partition barcodes. GEM reactions were thermally cycled (30  $^{\circ}$ C for 3 h and 65  $^{\circ}$ C for 10 min;  
475 held at 4  $^{\circ}$ C) and after amplification, the droplets were fractured. P5 and P7 primers, read 2,  
476 and sample index were added during library construction. The library was amplified using 10  
477 cycles of PCR and the DNA was subsequently size selected to 450 bp by performing a double

478 purification on AMPure Xp beads. Library quality was assessed using a Fragment Analyzer  
479 and quantified by qPCR using the Kapa Library Quantification Kit. Sequencing has been  
480 performed on an Illumina HiSeq3000 using a paired-end read length of 2x150 bp with the  
481 Illumina HiSeq3000 sequencing kits.

#### 482 ***Oxford nanopore genome sequencing***

483 High molecular weight gDNA purification steps were performed using AMPure XP beads  
484 (Beckman Coulter). Library preparation and sequencing were performed using Oxford  
485 Nanopore (Oxford Nanopore Technologies) Ligation Sequencing Kit SQK-LSK109 according  
486 to manufacturer's instructions "1D gDNA selecting for long reads (SQK-LSK109)". Five µg of  
487 DNA was purified then sheared at 20 kb using the megaruptor1 system (diagenode). A one-  
488 step DNA damage repair + END-repair + dA tail of double-stranded DNA fragments was  
489 performed on 2 µg of sample. Then adapters were ligated to the library. Library was loaded  
490 onto 1 R9.4.1 flowcell and sequenced on a PromethION instrument at 0.02 pM within 72 h.

#### 491 ***PacBio HiFi genome sequencing***

492 Library preparation and sequencing were performed according to the manufacturer's  
493 instructions "Procedure & Checklist Preparing HiFi SMRTbell Libraries using SMRTbell  
494 Express Template Prep Kit 2.0". Fifteen µg of DNA were purified and then sheared at 15 kb  
495 using the Megaruptor3 system (Diagenode). Using SMRTbell Express Template prep kit 2.0,  
496 a Single strand overhangs removal and then a DNA and END damage repair steps were  
497 performed on 10 µg of the sample. Then blunt hairpin adapters were ligated to the library. The  
498 library was treated with an exonuclease cocktail to digest unligated DNA fragments. A size  
499 selection step using a 12 kb cutoff was performed on the BluePippin Size Selection system  
500 (Sage Science) with "0.75% DF Marker S1 3-10 kb Improved Recovery" protocol. Using  
501 Binding kit 2.0 kit and sequencing kit 2.0, the primer V2 annealed and polymerase 2.0 bounded  
502 library was sequenced by diffusion loading onto 2 SMRTcells on Sequel2 instrument at 50 pM  
503 with a 2 h pre-extension and a 30 h movie.

#### 504 ***Hi-C sequencing***

505 Hi-C data was generated using the Arima-HiC kit (Ref. 510008), according to the  
506 manufacturer's protocols using 10 µl of blood as starting material, the Truseq DNA PCR-Free  
507 kit and Truseq DNA UD Indexes (Illumina, ref. 20015962, ref. 20020590), and the KAPA  
508 library Amplification kit (Roche, ref. KK2620). Hi-C library was sequenced in paired-end  
509 2x150 bp mode on Novaseq6000 (Illumina), using half a lane of a SP flow cell (ref. 20027464).

510 Image analyses and base calling were performed using the Illumina NovaSeq Control Software  
511 and Real-Time Analysis component (v3.4.4). Demultiplexing was performed using Illumina's  
512 conversion software (bcl2fastq v2.20). The quality of the raw data and potential contaminants  
513 was assessed using FastQC (v0.14.0)<sup>59</sup> from the Babraham Institute and the Illumina software  
514 SAV (Sequencing Analysis Viewer).

### 515 ***Genome assembly***

516 Pacbio HiFi reads were assembled with hifiasm<sup>60</sup> version 0.9 using standard parameters. The  
517 genome assembly fasta file was extracted from the principal gfa assembly graph file using an  
518 awk command line. This assembly was then scaffolded using Hi-C and 10X as a source of  
519 linking information. 10X reads were aligned using Long Ranger v2.1.1 (10x Genomics). Hi-C  
520 reads were aligned to the draft genome using Juicer<sup>61</sup> with default parameters. A candidate  
521 assembly was then generated with 3D de novo assembly (3D-DNA) pipeline<sup>62</sup> with the -r 0 and  
522 --polisher-input-size 100000 parameters. Finally, the candidate assembly was manually  
523 reviewed using the Juicebox assembly tools<sup>63</sup>. Due to the specific structure of the Pachón cave  
524 B chromosome, both Hi-C and 10X signals show some uncertainties in the order and  
525 orientation of the contigs. To improve the quality of the B chromosome assembly, ONT reads  
526 were then aligned to the final version of the genome using minimap2<sup>64</sup> v2.11 with -x map-ont  
527 parameter. Both reads spanning contig junctions and reads showing supplementary alignments  
528 linking contigs belonging to the B chromosome were analyzed to resolve these ambiguities.

### 529 ***Genome annotation***

530 The cavefish whole genome assembly was annotated using a pipeline adapted from previous  
531 studies<sup>65,66</sup>. In brief, RepeatModeler, RepeatProteinMask, and RepeatMasker (open-4.0.7,  
532 <http://www.repeatmasker.org/>) were first used to scan the genome and mask out repeats. Then  
533 protein-coding genes were annotated by collecting gene evidence from homology alignment,  
534 RNA-seq mapping, and *ab initio* prediction. For homology alignment, 464,144 protein  
535 sequences collected from NCBI were aligned to the assembly using Genewise<sup>67</sup> and Exonerate  
536 respectively. RNA-seq data were mapped to the assembly in two independent parallel steps.  
537 First Hisat<sup>68</sup> was used to align RNA-seq reads and then StringTie<sup>69</sup> was used to predict the gene  
538 models; in the other step reads were first assembled into transcript sequences using Trinity<sup>70</sup>  
539 and then PASA<sup>71</sup> was used to map the transcripts to the assembly and model the gene structures.  
540 For *ab initio* prediction and final integrating, Augustus<sup>72</sup> was first trained using the high-quality  
541 gene models and then ran in a hint-guide model.

542

### 543 ***B chromosome annotation***

544 First, repeats were identified and masked from the B chromosome using RepeatModeler,  
545 RepeatProteinMask, and RepeatMasker (open-4.0.7, <http://www.repeatmasker.org/>). To  
546 annotate protein-coding genes, we collected all protein sequences of *A. mexicanus* annotated  
547 by NCBI (Genome ID: 13073) and Ensembl (release-104), and aligned them onto the repeat-  
548 masked B sequence using GeneWise<sup>67,73</sup> and Exonerate respectively. For each query, the best  
549 hit was kept. To determine the best gene model when multiple ones compete for a splice site,  
550 we introduced RNA-seq data to evaluate the quality of these homology gene models. Hence  
551 RNA-seq data of *A. mexicanus* from the previous study<sup>74</sup> were aligned to B using HISAT<sup>68</sup> and  
552 parsed using StringTie<sup>69</sup>. RNA-score of each homology gene model was then calculated as the  
553 match-extend of splice sites to that of StringTie prediction. When multiple homology gene  
554 models compete for a splice site, those with lower RNA-score were discarded. In cases when  
555 some genes failed to be identified using homology alignment, we also implemented an *ab initio*  
556 gene prediction using Augustus<sup>72</sup>, where all the homology and transcriptome evidence were  
557 used as hints. The predicted results were included into the final gene set if 1) the splice sites  
558 are not occupied and 2) the splice sites match 100% to that of StringTie predictions (RNA-  
559 score =100). To further evaluate the quality of the final gene set, we blasted their protein  
560 sequences to SWISSPROT (<https://www.uniprot.org/>) and NR  
561 (<https://www.ncbi.nlm.nih.gov/>), and took the alignment to the best hit to check how much of  
562 the query and subject was aligned, respectively (query coverage & subject coverage). Genes  
563 with query and subject coverage both >90% were considered as being of good quality.  
564 To characterize the A chromosome content of the B chromosome, sequences of the B  
565 chromosome assembly were aligned to the sequences of the 25 A chromosomes with  
566 minimap2<sup>64</sup> (v2.11) and the best match of each contig fragment was retained. Overlapping  
567 matches were manually filtered considering match lengths and similarities (cigarline and edit  
568 distance) in order to build the best non-overlapping matching list. Karyoplots were then plotted  
569 using the R package karyoploteR<sup>75</sup> ([https://bernatgel.github.io/karyoploteR\\_tutorial/](https://bernatgel.github.io/karyoploteR_tutorial/)). The  
570 median, minimum, and maximum sizes of the 628 B best matches on A chromosomes were  
571 respectively 1,087 bp, 44 bp and 41,908 bp.

### 572 ***Male and female Pool-sequencing***

573 DNA was collected from 91 phenotypic Pachón cave males and 81 phenotypic Pachón cave  
574 females and was pooled as male and female pools separately. Before pooling, the DNA  
575 concentration was normalized in order to obtain an equal amount of each individual genome in

576 the final pool. Pool-sequencing libraries were prepared using the Illumina TruSeq Nano DNA  
577 HT Library Prep Kit (Illumina, San Diego, CA) according to the manufacturer's protocol. After  
578 the fragmentation of each gDNA pool (200 ng/pool) by sonication using an M220 Focused-  
579 ultrasonicator (COVARIS), the size selection was performed using SPB beads retaining  
580 fragments of 550 bp. Following the 3' ends of blunt fragments mono-adenylation and the  
581 ligation to specific paired-end adaptors, the amplification of the construction was performed  
582 using Illumina-specific primers. Library quality was verified with a Fragment Analyzer  
583 (Advanced Analytical Technologies) and then quantified by qPCR using the Kapa Library  
584 Quantification Kit (Roche Diagnostics Corp, Indianapolis, IN). The enriched male and female  
585 pool libraries were then sequenced using a paired-end multiplexed sequencing mode on a  
586 NovaSeq S4 lane (Illumina, San Diego, CA), combining the two pools on the same lane and  
587 producing 2×150 bp with Illumina NovaSeq Reagent Kits according to the manufacturer's  
588 instructions. Sequencing produced 288 million paired reads and 267 million paired reads for  
589 the male and female pool libraries, respectively.

#### 590 *Pool-sequencing analysis*

591 Characterization of genomic regions enriched for sex-biased signals between Pachón cave  
592 males and females, consisting of coverage and Single Nucleotide Variations (SNVs) was  
593 performed as described previously<sup>38,43</sup>. Pachón cave *A. mexicanus* paired-end reads from male  
594 and female pool-seq pools were mapped onto our own Pachón cave genome assembly using  
595 BWA mem version 0.7.17<sup>76</sup>. The resulting BAM files were sorted and the duplicate reads due  
596 to PCR amplification during library preparation were removed using Picard tools version  
597 2.18.2 (<http://broadinstitute.github.io/picard>) with default parameters. Then, for each pool and  
598 each genomic position, a file containing the nucleotide composition was generated using  
599 samtools mpileup<sup>77</sup> version 1.8, and popoolation2<sup>78</sup> mpileup2sync version 1201. This file was  
600 then analyzed with custom software (PSASS version 2.0.0; doi: 10.5281/zenodo.2615936) to  
601 compute: (a) the position and density of sex-specific SNVs, defined as SNVs heterozygous in  
602 one sex but homozygous in the other, and (b) the average read depths for male and female pools  
603 along the genome to look for regions present in one sex but absent in the other (i.e., sex-specific  
604 insertions). All PSASS analyses were run with default parameters except for the range of  
605 frequency for a sex-linked SNV in the homogametic sex, --range-hom, that was set to 0.01  
606 instead of 0.05, and the size of the sliding window, --window-size, that was set at 50,000  
607 instead of 100,000.

608 ***Chromosome conventional cytogenetics***

609 Mitotic or meiotic chromosome spreads were obtained either from regenerating caudal fin  
610 tissue as previously described<sup>79</sup>, with slight modifications<sup>80</sup> and altered time of fin regeneration  
611 (one week), or by direct preparation from the cephalic kidney and gonads<sup>81</sup>. In the latter, the  
612 quality of chromosomal spreading was enhanced by a previously described dropping method<sup>82</sup>.  
613 Chromosomes were stained with 5% Giemsa solution (pH 6.8) (Merck, Darmstadt, Germany)  
614 for conventional cytogenetic analyses, or left unstained for other methods. For FISH, slides  
615 were dehydrated in an ethanol series (70%, 80% and 96%, 3 min each) and stored at -20 °C  
616 before analysis. Constitutive heterochromatin was visualized by C-banding<sup>83</sup>, with  
617 chromosomes being counterstained by 4',6-diamidino-2-phenolindole (DAPI), 1.5 µg/ml in  
618 antifade (Cambio, Cambridge, United Kingdom).

619 ***gdf6b probe synthesis for FISH mapping***

620 gDNA was extracted using NucleoSpin Kits for Tissue (Macherey-Nagel, Duren, Germany) as  
621 described above. A *gdf6b* fragment comprising the two exons, the intron and 2,260 bp of the  
622 proximal promoter (with a total size of 4,368 bp) was amplified by PCR in a total volume of  
623 50 µl. The mixture contained 0.5 µM of each primer, a final concentration of 20 ng/µl gDNA,  
624 1X of 10X AccuPrime™ PCR Buffer II, 1U/reaction of AccuPrime™ Taq DNA Polymerase,  
625 High Fidelity (Thermofisher), was adjusted to 50 µl with autoclaved and distilled water.  
626 Cycling conditions were as follows: 94 °C for 45 sec, then 35 cycles of (94 °C for 15 sec + 64  
627 °C for 30 sec + 68 °C for 5 min and 30 sec), and 68 °C for 5 min. The resulting PCR product  
628 was cloned into TOPO TA cloning Kit XL (Thermofisher) and after sequence verification it  
629 was purified using NucleoSpin plasmid DNA purification kit (Machery-Nagel, Düren,  
630 Germany) according to the supplier's indications. This Pachón cave *gdf6b* cloned DNA  
631 fragment was labeled by nick translation with Cy3-dUTP using Cy3 NT Labeling Kit (Jena  
632 Bioscience, Jena, Germany). The optimal fragment size of the probe (approx. 200-500 bp) was  
633 achieved after 30 min of incubation at 15 °C.

634 ***Chromosome microdissection and FISH mapping***

635 Twelve copies of B chromosome from *A. mexicanus* male individual (male 10) and twelve  
636 copies encompassing two B chromosomes (per cell) from a male individual (male 9) were  
637 manually microdissected as previously described<sup>84</sup> under an inverted microscope (Zeiss  
638 Axiovert 135) using a sterile glass needle attached to a mechanical micromanipulator (Zeiss).  
639 The chromosomes were subsequently amplified by degenerate oligonucleotide primed-PCR

640 (DOP-PCR) following previously described protocols<sup>85</sup>. One  $\mu$ l of the resulting amplification  
641 product was used as a template DNA for a labeling DOP-PCR reaction, with Spectrum Orange-  
642 dUTP and Spectrum Green-dUTP, for Male 9 (2B) and Male 10 (1B), respectively (both Vysis,  
643 Downers Grove, USA). The amplification was done in 30 cycles, following previously  
644 described protocols<sup>86</sup>. Depending on the experimental scheme, the final probe mixture  
645 contained i) both painting probes (200 ng each) or ii) a single painting probe (200 ng) and a  
646 labeled 4,368 bp long fragment containing *gdf6b* gene and its promoter (300 ng; see below).  
647 To block the shared repetitive sequences, the probe also contained 4-5  $\mu$ g of unlabelled  
648 competitive DNA prepared from female gDNA (on male preparations) or male gDNA (on  
649 female preparations). Male and female gDNAs were isolated from liver and spleen using  
650 MagAttract HMW DNA kit (Qiagen) and C<sub>0</sub>t-1 DNA (i.e., fraction of gDNA enriched with  
651 highly and moderately repetitive sequences) was then generated from them according to  
652 previously described protocols<sup>87</sup>. The complete B probe mixture was dissolved in the final  
653 volume 20  $\mu$ l (in case of two painting probes) or 14  $\mu$ l (in case of one painting probe and a  
654 *gdf6b* gene probe) of hybridization mixture (50% formamide and 10% dextran sulfate in 2 $\times$   
655 SSC).

#### 656 ***FISH and whole-chromosome painting***

657 The FISH (Fluorescence in situ hybridization on chromosomes) experiments were done using  
658 a combination of two previously published protocols<sup>80,88</sup>, with slight modifications. Briefly,  
659 the aging of slides took place overnight at 37 °C and then 60 min at 60 °C, followed by  
660 treatments with RNase A (200  $\mu$ g/ml in 2 $\times$  SSC, 60–90 min, 37 °C) (Sigma-Aldrich) and then  
661 pepsin (50  $\mu$ g/ml in 10 mM HCl, 3 min, 37 °C). Subsequently, the slides were incubated in 1%  
662 formaldehyde in PBS (10 min) to stabilize the chromatin structure. Denaturation of  
663 chromosomes was done in 75% formamide in 2 $\times$  SSC (pH 7.0) (Sigma-Aldrich) at 72 °C, for  
664 3 min. The hybridization mixture was denatured for 8 min (86 °C) and then pre-hybridized at  
665 37 °C for 45 min to outcompete the repetitive fraction. After application of the probe cocktail  
666 on the slide, the hybridization took place in a moist chamber at 37 °C for 72 h. Subsequently,  
667 non-specific hybridization was removed by post-hybridization washes: two times in 1 $\times$  SSC  
668 (pH 7.0) (65 °C, 5 min each) and once in 4 $\times$  SSC in 0.01% Tween 20 (42°C, 5 min). Slides  
669 were then washed in PBS (1 min), passed through an ethanol series, and mounted in antifade  
670 containing 1.5  $\mu$ g/ml DAPI (Cambio, Cambridge, United Kingdom).

#### 671 ***Synaptonemal complex immunostaining***



672 Pachytene chromosome spreads from two Pachón cave *A. mexicanus* males (male 2 and 4)  
673 were prepared from testes following the protocol for *Danio rerio*<sup>89,90</sup> with some modifications.  
674 Briefly, dissected testes were suspended in 200-600 µl (based on the testes size and cell density)  
675 of cold PBS. Cell suspensions were applied onto poly-l-lysine slides (ThermoFisher), with 1:30  
676 (v/v) dilution in hypotonic solution (PBS: H<sub>2</sub>O, 1:2 v/v). After 20 min at room temperature  
677 (RT), slides were fixed with freshly prepared cold 2% formaldehyde (pH 8.0 – 8.5) for 3 min  
678 at RT. Slides were then washed three times in 0.1% Tween-20 (pH 8.0-8.5), 1 min each, and  
679 left to dry (1 h). Afterwards, immunofluorescence analysis of synaptonemal complexes took  
680 place, using antibodies against the proteins SYCP3 (lateral elements of synaptonemal  
681 complexes) and MLH1 (mismatch repair protein; marker for visualization of recombination  
682 sites). The primary antibodies – rabbit anti-SYCP3 (1:300; Abcam, Cambridge, UK) and  
683 mouse anti-MLH1 (1:50, Abcam) – were diluted (v/v) in 3% BSA (bovine serum albumin) in  
684 0.05% Triton X-100/ PBS. After application onto the slides, the incubation was carried out  
685 overnight in a humid chamber at 37°C. Next day, slides were washed three times in 0.1%  
686 Tween-20 in PBS, 10 min each and secondary antibodies, diluted (v/v) in 3% BSA (bovine  
687 serum albumin) in 0.05% Triton X-100/ PBS, were applied. Specifically, we used goat anti-  
688 rabbit Alexa 488 (1:300; Abcam) and goat anti-mouse Alexa555 (1:100; Abcam), and the slides  
689 were incubated for 3 h at 37 °C. Then, after washing in 0,1% Tween-20 in PBS (10 min) and  
690 brief washing in 0.01% Tween-20 in distilled H<sub>2</sub>O, slides were mounted in antifade containing  
691 DAPI, as described above.

### 692 ***Microscopy and image analysis***

693 At least 50 metaphase spreads per individual were analyzed to confirm the diploid chromosome  
694 number (2n), karyotype structure, and FISH results. Giemsa-stained preparations were  
695 analyzed under Axio Imager Z2 microscope (Zeiss, Oberkochen, Germany), equipped with an  
696 automatic Metafer-MSearch scanning platform. Photographs of the chromosomes were  
697 captured under 100× objective using CoolCube 1 b/w digital camera (MetaSystems,  
698 Altlussheim, Germany). The karyotypes were arranged using Ikaros software (MetaSystems,  
699 Altlussheim, Germany). Chromosomes were classified according to their centromere  
700 positions<sup>91</sup>, modified as metacentric (m), submetacentric (sm), subtelocentric (st), or  
701 acrocentric (a). FISH preparations were inspected using an Olympus BX53 epifluorescence  
702 microscope (Olympus, Tokyo, Japan), equipped with an appropriate fluorescence filter set.  
703 Black-and-white images were captured under 100× objective for each fluorescent dye with a  
704 cooled DP30BW CCD camera (Olympus) using Olympus Acquisition Software. The digital

705 images were then pseudo-colored (blue for DAPI, red for Cy3, green for FITC) and merged in  
706 DP Manager (Olympus). Composed images were then optimized and arranged using Adobe  
707 Photoshop CS6.

### 708 ***Phylogeny and synteny of Gdf6 proteins***

709 Phylogeny and synteny relationships of *Gdf6* genes were inferred from a Genomicus instance<sup>92</sup>  
710 in which synteny and phylogeny have been reconciled with the Scorpis pipeline<sup>93</sup> on 4  
711 tetrapod species, one sarcopterygii species, one holostei species and 13 teleosts (see Figure 3  
712 for species names).

### 713 ***Three-dimensional protein modelling***

714 Three-dimensional models for the proprotein of *A. mexicanus* A-Gdf6b and B-Gdf6b were  
715 obtained by homology modeling. The amino acid sequences of full-length A-Gdf6b and B-  
716 Gdf6b were submitted to automated homology modeling using the hm\_build macro of the  
717 software package YASARA<sup>94</sup>. Modeling includes alignment of the two target sequences  
718 against sequences from Uniprot *via* PSI-Blast to build a position-specific scoring function  
719 matrix/profile, which is then used to search the PDB structure data bank for suitable modeling  
720 targets. Five templates were identified with sufficiently high scores, i.e. PDB entries 4YCG  
721 (proprotein complex of GDF2 (alternative naming BMP9))<sup>95</sup>, 5HLY (proprotein complex of  
722 Activin A)<sup>96</sup>, 6Z3J (the mature C-terminal growth factor domain of GDF5 in complex with  
723 repulsive guidance molecule B)<sup>97</sup> as well as 6Z3M (which is like 6Z3J but includes neogenin  
724 in complex with GDF5 and the repulsive guidance molecule B)<sup>97</sup>, and 3QB4 (which is only the  
725 C-terminal growth factor domain of GDF5)<sup>98</sup>. Several initial models were built on the basis of  
726 these template structures, missing sequence elements were modeled in an automated procedure  
727 through YASARA on the basis of an indexed PDB structure database. By this scheme 13  
728 models were built, three only covered the C-terminal growth factor domain comprising residues  
729 293 to 398, while 10 models covered the proprotein complex consisting of residues 3 to 398  
730 (models on the basis of the 5HLY entry) and of residues 66 to 398 (models on the basis of  
731 template 4YCG). These models were individually refined by a short molecular dynamics  
732 simulation in explicit water to optimize hydrogen bonding and protein packing. Due to the  
733 overall low Z-score of the individual models, YASARA used the various models to form a  
734 hybrid homology model combining the elements with the highest-scoring factors into a single  
735 3D model. This hybrid model was then used for further analysis.

### 736 ***Expression analysis by Real- Time PCR***

737 For gene expression studies, mRNA transcripts levels were quantified during gonadal  
738 development from 10 dpf to 90 dpf, male and female gametogenesis stages, and finally in 10  
739 adult organs including gonads as described previously<sup>48</sup>. All samples were frozen in liquid  
740 nitrogen and stored at -80 °C until RNA extraction. Total RNA extraction from gonads, trunks,  
741 and adult organs, followed by cDNA synthesis, and expression analysis by RT-PCR were  
742 carried out as previously described<sup>48</sup>. Specific primers were designed for *gdf6b* in the most  
743 divergent sequence regions between the two paralogous *gdf6a* and *gdf6b* genes.

#### 744 ***RNAScope in situ hybridization of gdf6b***

745 RNA *in situ* hybridization (ISH) assays have been carried out using the RNAscope®  
746 technology (ACD Biotechnne™) on 7 µm cross-sections of 15, 21, 30 and 60 dpf Pachon  
747 cavefish fixed in paraformaldehyde 4% overnight at 4 °C and embedded in paraffin after serial  
748 dehydration in increasing methanol solutions. Specific probes for Pachon cavefish *gdf6b* and  
749 *gsdf* were synthesized by ACD Biotechnne™. Sections were collected on Super frost+ slides,  
750 heated at 60 °C for 1 h and dewaxed 2 x 5 min in xylene followed by 2x 2 min in Ethanol 100%  
751 at RT. Fluorescent ISH was carried out with the Multiplex Fluorescent Reagent Kit v2 (ACD  
752 Biotechnne™, ref: 323100) according to manufacturer's protocol. Following hybridization,  
753 nuclei were labelled with DAPI (4',6-diamidino-2-phenylindole) staining and slides were  
754 mounted with ProLong™ Gold Antifade Mountant (Invitrogen™) and observed with a Leica  
755 TCS SP8 laser scanning confocal microscope.

#### 756 ***Knockout of Pachón A. mexicanus gdf6b***

757 Pachón cave *A. mexicanus* inactivated for *gdf6b* were generated using the CRISPR/Cas9  
758 method. Guide RNAs (sgRNAs) targeting two sites located in exon 2 of *gdf6b* were designed  
759 using ZiFiT software<sup>99</sup> (<http://zifit.partners.org/ZiFiT/Disclaimer.aspx>). DR274 vector  
760 (Addgene #42250) containing the guide RNA universal sequence was first linearized with  
761 BsaI, electrophoresed in a 2% agarose gel and purified. PCR amplifications were then  
762 performed using linearized DR274 as a template and two primers for each sgRNA. Forward  
763 primers containing sgRNAs target sequences (#site 1 and #site 2) (bolded and underlined)  
764 between the T7 promoter sequence in the 5' end and the conserved tracrRNA domain sequence  
765 were as follows. Forward primer (#site 1): 5'-  
766 GAAATTAATACGACTCACTATAGGGAGTCTGAAACCGTTCTGGTTTTAGAGCTA  
767 GAAATAGCAAG-3'. Forward primer (#site 2): 5'-  
768 GAAATTAATACGACTCACTATAGGGGAGCTGGGCTGGGACGACGTTTTAGAGCT

769 AGAAATAGCAAG-3'. Universal Reverse primer: 5'-  
770 AAAAGCACCGACTCGGTGCCACT-3'. Subsequently, residual plasmid was digested with  
771 Dpn1 (renewed once) at 37°C for 3 hours. The final product was purified and used as a DNA  
772 template for transcription. The sgRNAs were transcribed using the MAXIscript™ T7  
773 Transcription Kit (Ambion) according to the manufacturer's instructions. The sgRNAs were  
774 precipitated in 200 µl of isopropanol solution at -20°C, centrifuged and the supernatant was  
775 removed. The precipitated sgRNAs were resuspended in RNase-free water. The sgRNAs were  
776 co-injected with Cas9 protein. Synthesized RNAs were then injected into 1-cell stage *A.*  
777 *mexicanus* Pachón cave embryos at the following concentrations: 72 ng/µl for each sgRNA and  
778 216 ng/µl for the Cas9 protein (kindly provided by Tacgene, MNHN, Paris). Genotyping was  
779 performed on gDNA from caudal fin-clips of adult fishes. CRISPR-positive fish were screened  
780 for mutations using a set of PCR primers (P7-P8) (Figure S3A, Data S1E) flanking the sgRNAs  
781 target sites leading to a ~470 bp deletion on the exon 2 of the *gdf6b* genes (Figure S10). The  
782 genetic sex of the mutants was determined by specific primers (P5-P6) on the *gdf6b* promoter  
783 with gap/indel variation between *A-gdf6b* and *B-gdf6b* (see STAR methods above and Figure  
784 S3A).

### 785 ***Histology***

786 Gonads were fixed in Bouin's fixative solution for 48 h and then dehydrated serially in aqueous  
787 70% and 95% ethanol, ethanol/butanol (5:95), and butanol. Tissues were embedded in paraffin  
788 blocks that were cutted serially into 5 µm sections, and were stained with hematoxylin-eosin-  
789 safran (HES) (Microm Microtech, Brignais, France).

790

## 791 **QUANTIFICATION AND STATISTICAL ANALYSIS**

### 792 ***Statistical analyses***

793 For the sex genotyping marker based on the heterozygous and specific site of the B  
794 chromosome on the exon 2 (position 679 bp of the *B-gdf6b* CDS), the significance of the  
795 correlation between this polymorphism and the male phenotypic sex was tested with the  
796 Pearson's Chi-squared test with Yates' continuity correction. For gene expression, normality of  
797 data residuals, homogeneity of variances and homoscedasticity were verified before  
798 performing parametric or non-parametric tests. Consequently, statistical analyses were carried  
799 out only with non-parametric tests using RStudio (Open Source version) considering the level

800 of significance at  $p < 0.05$ . For comparisons between two groups, we used Wilcoxon signed rank  
801 test. All data are shown as Mean  $\pm$  Standard Error of the Mean (SEM).  
802

## 803 LEGEND OF SUPPLEMENTARY DATAFILE

804 **Data S1: Supplementary information on metaphase numbers (A), genome assembly**  
805 **metrics and annotation (B, C, D), primer names (E) and sex linkage of B-gdf6b (F) in**  
806 **Pachón cavefish. Related to STAR Methods and Figures 1 and 2. A) Description of Data**  
807 **S1A.** Number of metaphases (NM) containing B chromosomes (Bs) in males and females of  
808 Pachón cave *A. mexicanus*. % M = percentage of metaphases. Only very few male metaphases  
809 did not have a B. In contrast, Bs were not detected in most females (7/11), and when present in  
810 females (4/11), they were detected only in very few metaphases and most often as a unique B  
811 copy. **B) Description of Data S1B.** Genome assembly metrics of the Pachón cavefish *A.*  
812 *mexicanus* male assembly (HiFi PacBio) and comparison with previous publicly available  
813 surface (*Astyanax\_mexicanus*-2.0) and Pachón cave (*Astyanax\_mexicanus*-1.02) genome  
814 assemblies. **C) Description of Data S1C.** Gene annotation of Pachón cavefish B chromosome.  
815 **D) Description of Data S1D.** Transposable elements in the Pachón cavefish genome. **E)**  
816 **Description of Data S1E.** Primer names, sequences, target genes, and their corresponding  
817 experiments. **F) Description of Data S1F.** Association between *B-gdf6b* specific  
818 amplifications and sex phenotypes with different *B-gdf6b* primer sets in a laboratory stock and  
819 in wild-caught Pachón cavefish. P-value of *B-gdf6b* association with sex is based on the  
820 Pearson's Chi-squared test with Yates' continuity correction.

821

## 822 REFERENCES

823

- 824 1. Wright, A.E., Dean, R., Zimmer, F., and Mank, J.E. (2016). How to make a sex chromosome.  
825 Nature Communications 7, 12087.
- 826 2. Furman, B.L.S., Metzger, D.C.H., Darolti, I., Wright, A.E., Sandkam, B.A., Almeida, P., Shu,  
827 J.J., and Mank, J.E. (2020). Sex Chromosome Evolution: So Many Exceptions to the Rules. Genome  
828 Biology and Evolution 12, 750–763.
- 829 3. D'Ambrosio, U., Alonso-Lifante, M.P., Barros, K., Kovařík, A., Xaxars, G.M. de, and Garcia,  
830 S. (2017). B-chrom: a database on B-chromosomes of plants, animals and fungi. New Phytologist 216,  
831 635–642.
- 832 4. Jones, N. (2017). New species with B chromosomes discovered since 1980. Nucleus 60, 263–  
833 281.
- 834 5. Camacho, J.P.M. (2005). CHAPTER 4 - B Chromosomes. In The Evolution of the Genome, T.  
835 R. Gregory, ed. (Academic Press), pp. 223–286.
- 836 6. Camacho, J.P.M., Sharbel, T.F., and Beukeboom, L.W. (2000). B-chromosome evolution.  
837 Philosophical Transactions of the Royal Society of London. Series B: Biological Sciences 355, 163–  
838 178.
- 839 7. Beladjal, L., Vandekerckhove, T.T.M., Muysen, B., Heyrman, J., de Caesemaeker, J., and  
840 Mertens, J. (2002). B-chromosomes and male-biased sex ratio with paternal inheritance in the fairy

841 shrimp *Branchipus schaefferi* (Crustacea, Anostraca). *Heredity* (Edinb) 88, 356–360.

842 8. Favarato, R.M., Ribeiro, L.B., Ota, R.P., Nakayama, C.M., and Feldberg, E. (2019).  
843 Cytogenetic Characterization of Two *Metynnis* Species (Characiformes, Serrasalminidae) Reveals B  
844 Chromosomes Restricted to the Females. *CGR* 158, 38–45.

845 9. Néo, D.M., Filho, O.M., and Camacho, J.P.M. (2000). Altitudinal variation for B chromosome  
846 frequency in the characid fish *Astyanax scabripinnis*. *Heredity* 85, 136–141.

847 10. Vicente, V.E., Moreira-Filho, O., and Camacho, J.P. (1996). Sex-ratio distortion associated  
848 with the presence of a B chromosome in *Astyanax scabripinnis* (Teleostei, Characidae). *Cytogenet Cell*  
849 *Genet* 74, 70–75.

850 11. Stange, E. a. R., and Almeida-toledo, L.F. (1993). Supernumerary b chromosomes restricted to  
851 males in *astyanax scabripinnis* ( pisces , characidae ). *Revista brasileira de genetica* 16, 601–615.

852 12. Clark, F.E., Conte, M.A., Ferreira-Bravo, I.A., Poletto, A.B., Martins, C., and Kocher, T.D.  
853 (2017). Dynamic Sequence Evolution of a Sex-Associated B Chromosome in Lake Malawi Cichlid  
854 Fish. *Journal of Heredity* 108, 53–62.

855 13. Clark, F.E., and Kocher, T.D. (2019). Changing sex for selfish gain: B chromosomes of Lake  
856 Malawi cichlid fish. *Scientific Reports* 9, 20213.

857 14. Yoshida, K., Terai, Y., Mizoiri, S., Aibara, M., Nishihara, H., Watanabe, M., Kuroiwa, A.,  
858 Hirai, H., Hirai, Y., Matsuda, Y., et al. (2011). B Chromosomes Have a Functional Effect on Female  
859 Sex Determination in Lake Victoria Cichlid Fishes. *PLOS Genetics* 7, e1002203.

860 15. Camacho, J.P.M., Schmid, M., and Cabrero, J. (2011). B Chromosomes and Sex in Animals.  
861 *SXD* 5, 155–166.

862 16. Hanlon, S.L., and Hawley, R.S. (2018). B Chromosomes in the *Drosophila* Genus. *Genes*  
863 (Basel) 9.

864 17. Martis, M.M., Klemme, S., Banaei-Moghaddam, A.M., Blattner, F.R., Macas, J., Schmutzer,  
865 T., Scholz, U., Gundlach, H., Wicker, T., Šimková, H., et al. (2012). Selfish supernumerary  
866 chromosome reveals its origin as a mosaic of host genome and organellar sequences. *PNAS* 109, 13343–  
867 13346.

868 18. Valente, G.T., Conte, M.A., Fantinatti, B.E.A., Cabral-de-Mello, D.C., Carvalho, R.F., Vicari,  
869 M.R., Kocher, T.D., and Martins, C. (2014). Origin and evolution of B chromosomes in the cichlid fish  
870 *Astatotilapia latifasciata* based on integrated genomic analyses. *Mol Biol Evol* 31, 2061–2072.

871 19. Ahmad, S.F., Jehangir, M., Cardoso, A.L., Wolf, I.R., Margarido, V.P., Cabral-de-Mello, D.C.,  
872 O'Neill, R., Valente, G.T., and Martins, C. (2020). B chromosomes of multiple species have intense  
873 evolutionary dynamics and accumulated genes related to important biological processes. *BMC*  
874 *Genomics* 21, 656.

875 20. Pansonato-Alves, J.C., Serrano, É.A., Utsunomia, R., Camacho, J.P.M., da Costa Silva, G.J.,  
876 Vicari, M.R., Artoni, R.F., Oliveira, C., and Foresti, F. (2014). Single origin of sex chromosomes and  
877 multiple origins of B chromosomes in fish genus *Characidium*. *PLoS One* 9, e107169.

878 21. Serrano-Freitas, É.A., Silva, D.M.Z.A., Ruiz-Ruano, F.J., Utsunomia, R., Araya-Jaime, C.,  
879 Oliveira, C., Camacho, J.P.M., and Foresti, F. (2020). Satellite DNA content of B chromosomes in the  
880 characid fish *Characidium gomesi* supports their origin from sex chromosomes. *Mol Genet Genomics*  
881 295, 195–207.

882 22. Conte, M.A., Clark, F.E., Roberts, R.B., Xu, L., Tao, W., Zhou, Q., Wang, D., and Kocher,  
883 T.D. (2021). Origin of a Giant Sex Chromosome. *Molecular Biology and Evolution* 38, 1554–1569.

884 23. Zhou, Q., Zhu, H., Huang, Q., Zhao, L., Zhang, G., Roy, S.W., Vicoso, B., Xuan, Z., Ruan, J.,  
885 Zhang, Y., et al. (2012). Deciphering neo-sex and B chromosome evolution by the draft genome of  
886 *Drosophila albomicans*. *BMC Genomics* 13, 109.

887 24. Piscor, D., and Parise-Maltempi, P.P. (2016). Microsatellite Organization in the B Chromosome  
888 and A Chromosome Complement in *Astyanax* (Characiformes, Characidae) Species. *Cytogenet*

889 Genome Res 148, 44–51.

890 25. Kavalco, K.F., and De Almeida-Toledo, L.F. (2007). Molecular Cytogenetics of Blind Mexican  
891 Tetra and Comments on the Karyotypic Characteristics of Genus *Astyanax* (Teleostei, Characidae).  
892 Zebrafish 4, 103–111.

893 26. Ebrahimzadegan, R., Houben, A., and Mirzaghaderi, G. (2019). Repetitive DNA landscape in  
894 essential A and supernumerary B chromosomes of *Festuca pratensis* Huds. Scientific Reports 9, 19989.

895 27. Mizoguchi, S.M.H.N., and Martins-Santos, I.C. (1997). Macro- and Microchromosomes B in  
896 Females of *Astyanax scabripinnis* (Pisces, Characidae). Hereditas 127, 249–253.

897 28. Portela-Castro, A.L. de B., Júnior, H.F.J., and Nishiyama, P.B. (2000). New occurrence of  
898 microchromosomes B in *Moenkhausia sanctaefilomenae* (Pisces, Characidae) from the Paraná River of  
899 Brazil: analysis of the synaptonemal complex. Genetica 110, 277–283.

900 29. Houben, A. (2017). B Chromosomes – A Matter of Chromosome Drive. Front. Plant Sci. 8.

901 30. Jones, R.N., González-Sánchez, M., González-García, M., Vega, J.M., and Puertas, M.J.  
902 (2008). Chromosomes with a life of their own. Cytogenet Genome Res 120, 265–280.

903 31. McGaugh, S.E., Gross, J.B., Aken, B., Blin, M., Borowsky, R., Chalopin, D., Hinaux, H.,  
904 Jeffery, W.R., Keene, A., Ma, L., et al. (2014). The cavefish genome reveals candidate genes for eye  
905 loss. Nat Commun 5, 5307.

906 32. Ahmad, S.F., and Martins, C. (2019). The Modern View of B Chromosomes Under the Impact  
907 of High Scale Omics Analyses. Cells 8.

908 33. Blavet, N., Yang, H., Su, H., Solanský, P., Douglas, R.N., Karafiátová, M., Šimková, L., Zhang,  
909 J., Liu, Y., Hou, J., et al. (2021). Sequence of the supernumerary B chromosome of maize provides  
910 insight into its drive mechanism and evolution. Proc Natl Acad Sci U S A 118, e2104254118.

911 34. Navarro-Domínguez, B., Ruiz-Ruano, F.J., Cabrero, J., Corral, J.M., López-León, M.D.,  
912 Sharbel, T.F., and Camacho, J.P.M. (2017). Protein-coding genes in B chromosomes of the grasshopper  
913 *Eyprepocnemis plorans*. Sci Rep 7, 45200.

914 35. Ruiz-Ruano, F.J., Cabrero, J., López-León, M.D., Sánchez, A., and Camacho, J.P.M. (2018).  
915 Quantitative sequence characterization for repetitive DNA content in the supernumerary chromosome  
916 of the migratory locust. Chromosoma 127, 45–57.

917 36. Christoffels, A., Koh, E.G.L., Chia, J., Brenner, S., Aparicio, S., and Venkatesh, B. (2004).  
918 Fugu Genome Analysis Provides Evidence for a Whole-Genome Duplication Early During the  
919 Evolution of Ray-Finned Fishes. Molecular Biology and Evolution 21, 1146–1151.

920 37. Vandepoele, K., De Vos, W., Taylor, J.S., Meyer, A., and Van de Peer, Y. (2004). Major events  
921 in the genome evolution of vertebrates: Paraneome age and size differ considerably between ray-finned  
922 fishes and land vertebrates. Proc Natl Acad Sci U S A 101, 1638–1643.

923 38. Feron, R., Zahm, M., Cabau, C., Klopp, C., Roques, C., Bouchez, O., Eché, C., Valière, S.,  
924 Donnadiou, C., Haffray, P., et al. (2020). Characterization of a Y-specific duplication/insertion of the  
925 anti-Mullerian hormone type II receptor gene based on a chromosome-scale genome assembly of yellow  
926 perch, *Perca flavescens*. Mol Ecol Resour 20, 531–543.

927 39. Kamiya, T., Kai, W., Tasumi, S., Oka, A., Matsunaga, T., Mizuno, N., Fujita, M., Suetake, H.,  
928 Suzuki, S., Hosoya, S., et al. (2012). A trans-species missense SNP in *Amhr2* is associated with sex  
929 determination in the tiger pufferfish, *Takifugu rubripes* (fugu). PLoS Genet. 8, e1002798.

930 40. Rafati, N., Chen, J., Herpin, A., Pettersson, M.E., Han, F., Feng, C., Wallerman, O., Rubin, C.-  
931 J., Péron, S., Cocco, A., et al. (2020). Reconstruction of the birth of a male sex chromosome present in  
932 Atlantic herring. PNAS 117, 24359–24368.

933 41. Li, M., Sun, Y., Zhao, J., Shi, H., Zeng, S., Ye, K., Jiang, D., Zhou, L., Sun, L., Tao, W., et al.  
934 (2015). A Tandem Duplicate of Anti-Müllerian Hormone with a Missense SNP on the Y Chromosome  
935 Is Essential for Male Sex Determination in Nile Tilapia, *Oreochromis niloticus*. PLOS Genetics 11,  
936 e1005678.



- 937 42. Hattori, R.S., Murai, Y., Oura, M., Masuda, S., Majhi, S.K., Sakamoto, T., Fernandino, J.I.,  
938 Somoza, G.M., Yokota, M., and Strüssmann, C.A. (2012). A Y-linked anti-Müllerian hormone  
939 duplication takes over a critical role in sex determination. *Proc. Natl. Acad. Sci. U.S.A.* *109*, 2955–  
940 2959.
- 941 43. Pan, Q., Feron, R., Yano, A., Guyomard, R., Jouanno, E., Vigouroux, E., Wen, M., Busnel, J.-  
942 M., Bobe, J., Concordet, J.-P., et al. (2019). Identification of the master sex determining gene in  
943 Northern pike (*Esox lucius*) reveals restricted sex chromosome differentiation. *PLOS Genetics* *15*,  
944 e1008013.
- 945 44. Reichwald, K., Petzold, A., Koch, P., Downie, B.R., Hartmann, N., Pietsch, S., Baumgart, M.,  
946 Chalopin, D., Felder, M., Bens, M., et al. (2015). Insights into Sex Chromosome Evolution and Aging  
947 from the Genome of a Short-Lived Fish. *Cell* *163*, 1527–1538.
- 948 45. Gautier, A., Sohm, F., Joly, J.-S., Le Gac, F., and Lareyre, J.-J. (2011). The Proximal Promoter  
949 Region of the Zebrafish *gsdf* Gene Is Sufficient to Mimic the Spatio-Temporal Expression Pattern of  
950 the Endogenous Gene in Sertoli and Granulosa Cells<sup>1</sup>. *Biology of Reproduction* *85*, 1240–1251.
- 951 46. Nakamura, S., Kobayashi, D., Aoki, Y., Yokoi, H., Ebe, Y., Wittbrodt, J., and Tanaka, M.  
952 (2006). Identification and lineage tracing of two populations of somatic gonadal precursors in medaka  
953 embryos. *Dev. Biol.* *295*, 678–688.
- 954 47. Sawatari, E., Shikina, S., Takeuchi, T., and Yoshizaki, G. (2007). A novel transforming growth  
955 factor- $\beta$  superfamily member expressed in gonadal somatic cells enhances primordial germ cell and  
956 spermatogonial proliferation in rainbow trout (*Oncorhynchus mykiss*). *Developmental Biology* *301*,  
957 266–275.
- 958 48. Imarazene, B., Beille, S., Jouanno, E., Branthonne, A., Thermes, V., Thomas, M., Herpin, A.,  
959 Rétaux, S., and Guiguen, Y. (2021). Primordial Germ Cell Migration and Histological and Molecular  
960 Characterization of Gonadal Differentiation in Pachón Cavefish *Astyanax mexicanus*. *Sex Dev*, 1–18.
- 961 49. Benetta, E.D., Antoshechkin, I., Yang, T., Nguyen, H.Q.M., Ferree, P.M., and Akbari, O.S.  
962 (2020). Genome elimination mediated by gene expression from a selfish chromosome. *Science*  
963 *Advances* *6*, eaaz9808.
- 964 50. Nur, U., Werren, J.H., Eickbush, D.G., Burke, W.D., and Eickbush, T.H. (1988). A “selfish” B  
965 chromosome that enhances its transmission by eliminating the paternal genome. *Science* *240*, 512–514.
- 966 51. Jones, R.N. (2018). Transmission and Drive Involving Parasitic B Chromosomes. *Genes*  
967 (Basel) *9*, E388.
- 968 52. Bernardino, A.C.S., Cabral-de-Mello, D.C., Machado, C.B., Palacios-Gimenez, O.M., Santos,  
969 N., and Loreto, V. (2017). B Chromosome Variants of the Grasshopper *Xyleus discoideus angulatus*  
970 Are Potentially Derived from Pericentromeric DNA. *Cytogenet Genome Res* *152*, 213–221.
- 971 53. Stevens, J.P., and Bougourd, S.M. (1994). Unstable B-chromosomes in a European population  
972 of *Allium schoenoprasum* L. (Liliaceae). *Biological Journal of the Linnean Society* *52*, 357–363.
- 973 54. Ruban, A., Schmutzer, T., Wu, D.D., Fuchs, J., Boudichevskaia, A., Rubtsova, M., Pistrick, K.,  
974 Melzer, M., Himmelbach, A., Schubert, V., et al. (2020). Supernumerary B chromosomes of *Aegilops*  
975 *speltoides* undergo precise elimination in roots early in embryo development. *Nature Communications*  
976 *11*, 2764.
- 977 55. Hinaux, H., Pottin, K., Chalhoub, H., Père, S., Elipot, Y., Legendre, L., and Rétaux, S. (2011).  
978 A developmental staging table for *Astyanax mexicanus* surface fish and Pachón cavefish. *Zebrafish* *8*,  
979 155–165.
- 980 56. Elipot, Y., Legendre, L., Père, S., Sohm, F., and Rétaux, S. (2014). *Astyanax* transgenesis and  
981 husbandry: how cavefish enters the laboratory. *Zebrafish* *11*, 291–299.
- 982 57. Gharbi, K., Gautier, A., Danzmann, R.G., Gharbi, S., Sakamoto, T., Høyheim, B., Taggart, J.B.,  
983 Cairney, M., Powell, R., Krieg, F., et al. (2006). A linkage map for brown trout (*Salmo trutta*):  
984 chromosome homeologies and comparative genome organization with other salmonid fish. *Genetics*

985 172, 2405–2419.

986 58. Köressaar, T., Lepamets, M., Kaplinski, L., Raime, K., Andreson, R., and Remm, M. (2018).

987 Primer3\_masker: integrating masking of template sequence with primer design software.

988 *Bioinformatics* 34, 1937–1938.

989 59. Wingett, S.W., and Andrews, S. (2018). FastQ Screen: A tool for multi-genome mapping and

990 quality control. *F1000Res* 7.

991 60. Cheng, H., Concepcion, G.T., Feng, X., Zhang, H., and Li, H. (2021). Haplotype-resolved de

992 novo assembly using phased assembly graphs with hifiasm. *Nat Methods* 18, 170–175.

993 61. Durand, N.C., Shamim, M.S., Machol, I., Rao, S.S.P., Huntley, M.H., Lander, E.S., and Aiden,

994 E.L. (2016). Juicer Provides a One-Click System for Analyzing Loop-Resolution Hi-C Experiments.

995 *Cell Syst* 3, 95–98.

996 62. Dudchenko, O., Batra, S.S., Omer, A.D., Nyquist, S.K., Hoeger, M., Durand, N.C., Shamim,

997 M.S., Machol, I., Lander, E.S., Aiden, A.P., et al. (2017). De novo assembly of the *Aedes aegypti*

998 genome using Hi-C yields chromosome-length scaffolds. *Science* 356, 92–95.

999 63. Durand, N.C., Robinson, J.T., Shamim, M.S., Machol, I., Mesirov, J.P., Lander, E.S., and

1000 Aiden, E.L. (2016). Juicebox Provides a Visualization System for Hi-C Contact Maps with Unlimited

1001 Zoom. *cels* 3, 99–101.

1002 64. Li, H. (2018). Minimap2: pairwise alignment for nucleotide sequences. *Bioinformatics* 34,

1003 3094–3100.

1004 65. Powell, D.L., García-Olazábal, M., Keegan, M., Reilly, P., Du, K., Díaz-Loyo, A.P., Banerjee,

1005 S., Blakkan, D., Reich, D., Andolfatto, P., et al. (2020). Natural hybridization reveals incompatible

1006 alleles that cause melanoma in swordtail fish. *Science* 368, 731–736.

1007 66. Du, K., Stöck, M., Kneitz, S., Klopp, C., Woltering, J.M., Adolffi, M.C., Feron, R., Prokopov,

1008 D., Makunin, A., Kichigin, I., et al. (2020). The sterlet sturgeon genome sequence and the mechanisms

1009 of segmental rediploidization. *Nat Ecol Evol* 4, 841–852.

1010 67. Birney, E., Clamp, M., and Durbin, R. (2004). GeneWise and Genomewise. *Genome Res* 14,

1011 988–995.

1012 68. Kim, D., Langmead, B., and Salzberg, S.L. (2015). HISAT: a fast spliced aligner with low

1013 memory requirements. *Nat Methods* 12, 357–360.

1014 69. Pertea, M., Pertea, G.M., Antonescu, C.M., Chang, T.-C., Mendell, J.T., and Salzberg, S.L.

1015 (2015). StringTie enables improved reconstruction of a transcriptome from RNA-seq reads. *Nat*

1016 *Biotechnol* 33, 290–295.

1017 70. Grabherr, M.G., Haas, B.J., Yassour, M., Levin, J.Z., Thompson, D.A., Amit, I., Adiconis, X.,

1018 Fan, L., Raychowdhury, R., Zeng, Q., et al. (2011). Full-length transcriptome assembly from RNA-Seq

1019 data without a reference genome. *Nat Biotechnol* 29, 644–652.

1020 71. Haas, B.J., Delcher, A.L., Mount, S.M., Wortman, J.R., Smith, R.K., Hannick, L.I., Maiti, R.,

1021 Ronning, C.M., Rusch, D.B., Town, C.D., et al. (2003). Improving the *Arabidopsis* genome annotation

1022 using maximal transcript alignment assemblies. *Nucleic Acids Res* 31, 5654–5666.

1023 72. Stanke, M., Keller, O., Gunduz, I., Hayes, A., Waack, S., and Morgenstern, B. (2006).

1024 AUGUSTUS: ab initio prediction of alternative transcripts. *Nucleic Acids Res* 34, W435–439.

1025 73. She, R., Chu, J.S.-C., Wang, K., Pei, J., and Chen, N. (2009). GenBlastA: enabling BLAST to

1026 identify homologous gene sequences. *Genome Res* 19, 143–149.

1027 74. Pasquier, J., Cabau, C., Nguyen, T., Jouanno, E., Severac, D., Braasch, I., Journot, L.,

1028 Pontarotti, P., Klopp, C., Postlethwait, J.H., et al. (2016). Gene evolution and gene expression after

1029 whole genome duplication in fish: the PhyloFish database. *BMC Genomics* 17, 368.

1030 75. Gel, B., and Serra, E. (2017). karyoploteR: an R/Bioconductor package to plot customizable

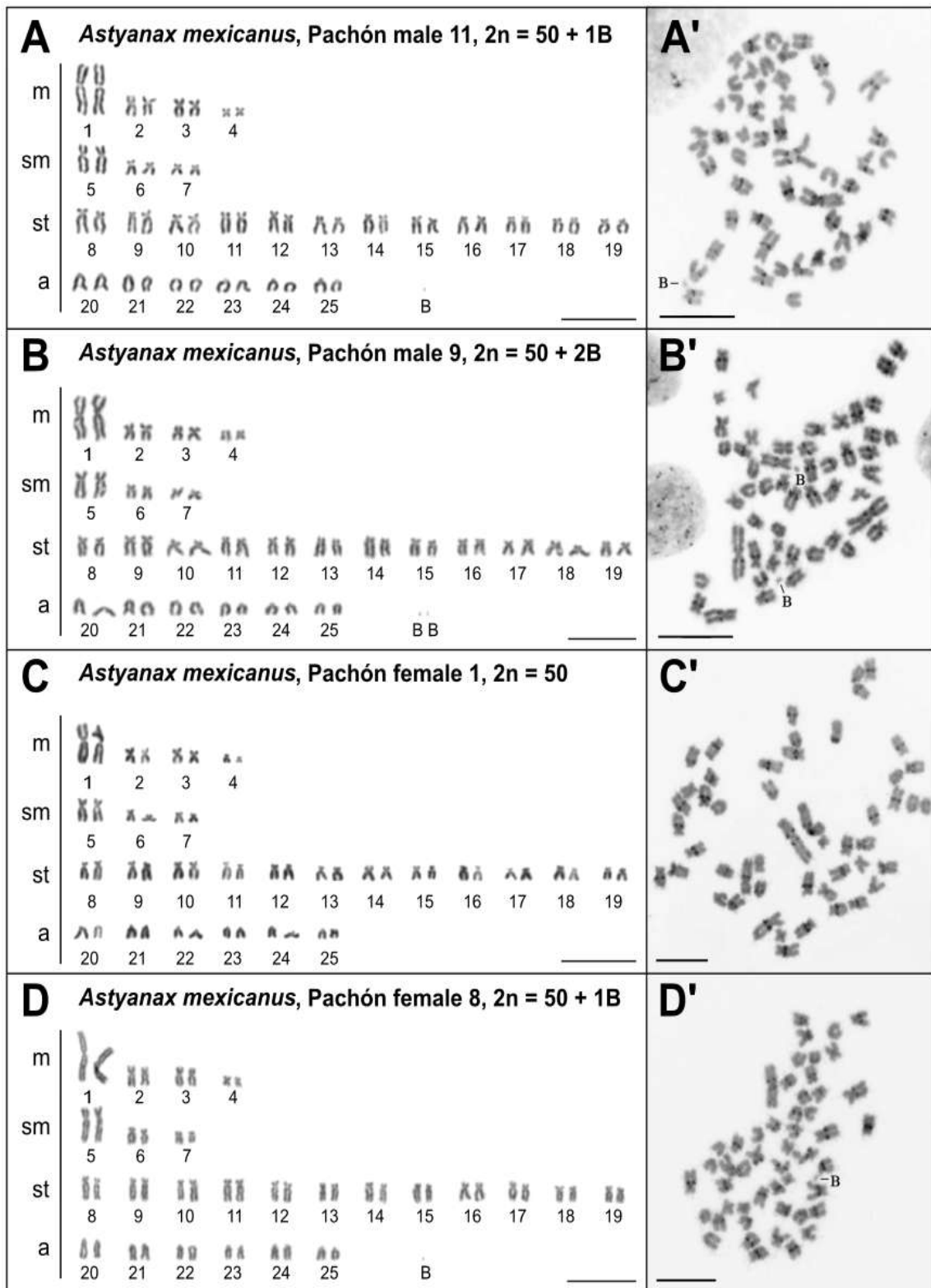
1031 genomes displaying arbitrary data. *Bioinformatics* 33, 3088–3090.

1032 76. Li, H. (2013). Aligning sequence reads, clone sequences and assembly contigs with BWA-

- 1033 MEM.
- 1034 77. Li, H., Handsaker, B., Wysoker, A., Fennell, T., Ruan, J., Homer, N., Marth, G., Abecasis, G.,  
1035 Durbin, R., and 1000 Genome Project Data Processing Subgroup (2009). The Sequence Alignment/Map  
1036 format and SAMtools. *Bioinformatics* 25, 2078–2079.
- 1037 78. Kofler, R., Pandey, R.V., and Schlötterer, C. (2011). PoPoolation2: identifying differentiation  
1038 between populations using sequencing of pooled DNA samples (Pool-Seq). *Bioinformatics* 27, 3435–  
1039 3436.
- 1040 79. Völker, M., and Ráb, P. (2015). Direct Chromosome Preparations from Embryos and Larvae.  
1041 In *Fish Cytogenetic Techniques* (CRC Press), p. 7.
- 1042 80. Sember, A., Bohlen, J., Šlechtová, V., Altmanová, M., Symonová, R., and Ráb, P. (2015).  
1043 Karyotype differentiation in 19 species of river loach fishes (Nemacheilidae, Teleostei): extensive  
1044 variability associated with rDNA and heterochromatin distribution and its phylogenetic and ecological  
1045 interpretation. *BMC Evol Biol* 15, 251.
- 1046 81. Ráb, P., and Roth, P. (1988). Cold-blooded vertebrates. In *Methods of Chromosome Analysis*  
1047 (Czechoslovak Biological Society Publishers), pp. 115–124.
- 1048 82. Bertollo, L., Cioffi, M., and Moreira-Filho, O. (2015). Direct Chromosome Preparation from  
1049 Freshwater Teleost Fishes (CRC Press).
- 1050 83. Haaf, T., and Schmid, M. (1984). An early stage of ZW/ZZ sex chromosome differentiation in  
1051 *Poecilia sphenops* var. *melanistica* (Poeciliidae, Cyprinodontiformes). *Chromosoma* 89, 37–41.
- 1052 84. Ahmed, A.-R., Leon, B.L., and Thomas, L. (2020). Glass needle-based chromosome  
1053 microdissection—How to set up probes for molecular cytogenetics? *Video Journal of Clinical Research*  
1054 2, 1.
- 1055 85. Yang, F., Trifonov, V., Ng, B.L., Kosyakova, N., and Carter, N.P. (2009). Generation of Paint  
1056 Probes by Flow-Sorted and Microdissected Chromosomes. In *Fluorescence In Situ Hybridization*  
1057 (FISH) — Application Guide Springer Protocols Handbooks., T. Liehr, ed. (Springer), pp. 35–52.
- 1058 86. Yang, F., and Graphodatsky, A.S. (2009). Animal Probes and ZOO-FISH. In *Fluorescence In*  
1059 *Situ Hybridization (FISH) — Application Guide Springer Protocols Handbooks.*, T. Liehr, ed.  
1060 (Springer), pp. 323–346.
- 1061 87. Zwick, M.S., Hanson, R.E., Islam-Faridi, M.N., Stelly, D.M., Wing, R.A., Price, H.J., and  
1062 McKnight, T.D. (1997). A rapid procedure for the isolation of C0t-1 DNA from plants. *Genome* 40,  
1063 138–142.
- 1064 88. Yano, C.F., Bertollo, L. a. C., Ezaz, T., Trifonov, V., Sember, A., Liehr, T., and Cioffi, M.B.  
1065 (2017). Highly conserved Z and molecularly diverged W chromosomes in the fish genus *Triportheus*  
1066 (Characiformes, Triporthidae). *Heredity (Edinb)* 118, 276–283.
- 1067 89. Kochakpour, N. (2009). Immunofluorescent microscopic study of meiosis in zebrafish.  
1068 *Methods Mol Biol* 558, 251–260.
- 1069 90. Kochakpour, N., and Moens, P.B. (2008). Sex-specific crossover patterns in Zebrafish (*Danio*  
1070 *rerio*). *Heredity* 100, 489–495.
- 1071 91. Levan, A., Fredga, K., and Sandberg, A.A. (1964). Nomenclature for Centromeric Position on  
1072 Chromosomes. *Hereditas* 52, 201–220.
- 1073 92. Louis, A., Muffato, M., and Roest Crollius, H. (2013). Genomicus: five genome browsers for  
1074 comparative genomics in eukaryota. *Nucleic Acids Res.* 41, D700-705.
- 1075 93. Parey, E., Louis, A., Cabau, C., Guiguen, Y., Crollius, H.R., and Berthelot, C. (2020). Synten-  
1076 y-guided resolution of gene trees clarifies the functional impact of whole genome duplications. *Mol. Biol.*  
1077 *Evol.*
- 1078 94. Krieger, E., and Vriend, G. (2014). YASARA View—molecular graphics for all devices—from  
1079 smartphones to workstations. *Bioinformatics* 30, 2981–2982.
- 1080 95. Mi, L.-Z., Brown, C.T., Gao, Y., Tian, Y., Le, V.Q., Walz, T., and Springer, T.A. (2015).

1081 Structure of bone morphogenetic protein 9 procomplex. *Proc Natl Acad Sci U S A* *112*, 3710–3715.  
1082 96. Wang, X., Fischer, G., and Hyvönen, M. (2016). Structure and activation of pro-activin A. *Nat*  
1083 *Commun* *7*, 12052.  
1084 97. Malinauskas, T., Peer, T.V., Bishop, B., Mueller, T.D., and Siebold, C. (2020). Repulsive  
1085 guidance molecules lock growth differentiation factor 5 in an inhibitory complex. *PNAS* *117*, 15620–  
1086 15631.  
1087 98. Klammert, U., Mueller, T.D., Hellmann, T.V., Wuerzler, K.K., Kotsch, A., Schliermann, A.,  
1088 Schmitz, W., Kuebler, A.C., Sebald, W., and Nickel, J. (2015). GDF-5 can act as a context-dependent  
1089 BMP-2 antagonist. *BMC Biol* *13*, 77.  
1090 99. Sander, J.D., Maeder, M.L., Reyon, D., Voytas, D.F., Joung, J.K., and Dobbs, D. (2010). ZiFiT  
1091 (Zinc Finger Targeter): an updated zinc finger engineering tool. *Nucleic Acids Res* *38*, W462-468.  
1092 100. Hwang, W.Y., Fu, Y., Reyon, D., Maeder, M.L., Tsai, S.Q., Sander, J.D., Peterson, R.T., Yeh,  
1093 J.-R.J., and Joung, J.K. (2013). Efficient genome editing in zebrafish using a CRISPR-Cas system. *Nat*  
1094 *Biotechnol* *31*, 227–229.  
1095 101. Li, H. (2013). Aligning sequence reads, clone sequences and assembly contigs with BWA-  
1096 MEM. arXiv:1303.3997 [q-bio].  
1097  
1098

## Supplementary figures



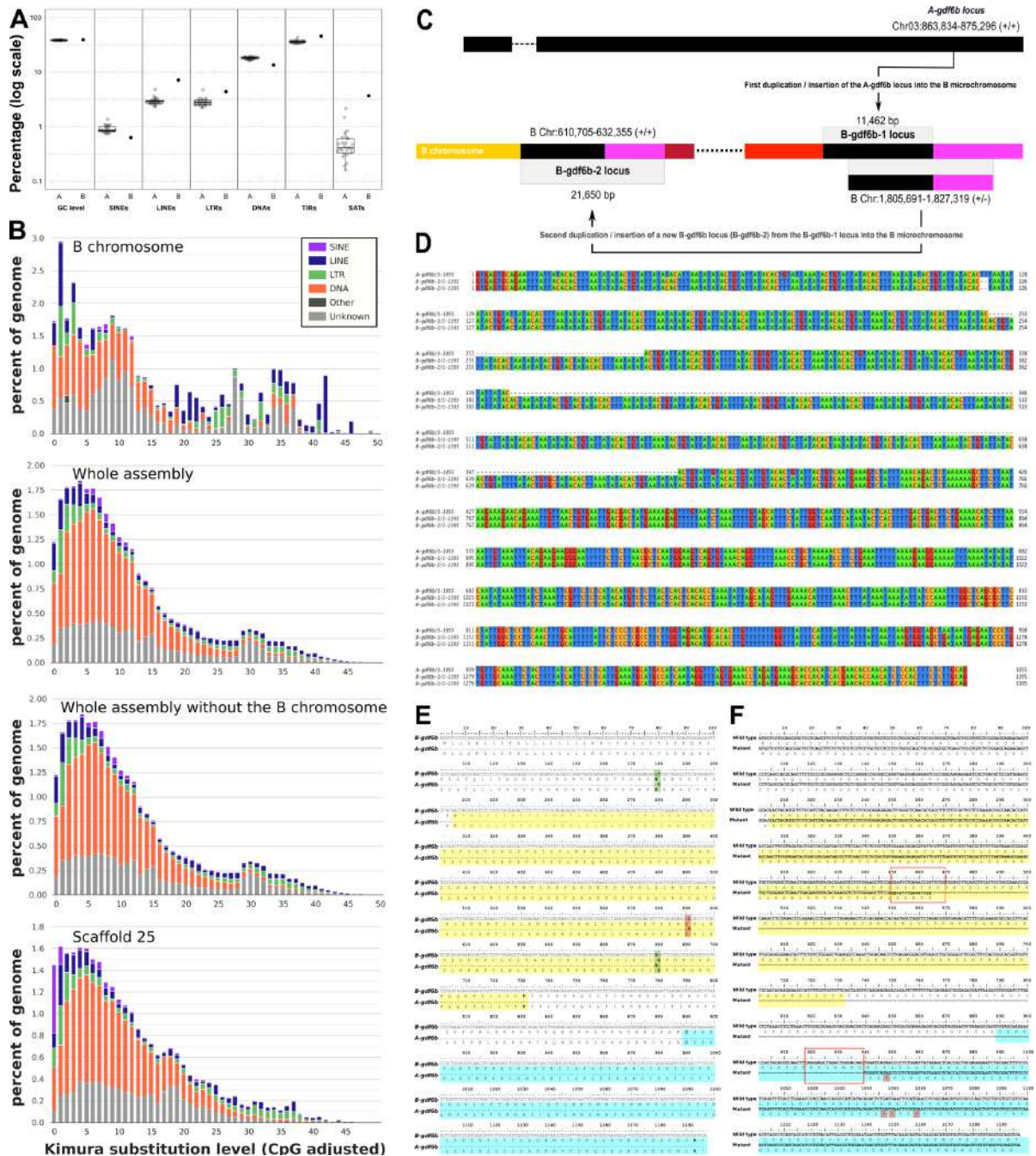
1100

1101

1102 **Figure S1. Karyotypes and corresponding C-banded mitotic metaphases of Pachón cave**1103 *Astyanax mexicanus*, with different male and female B chromosome (B) constitution.1104 **Related to Figure 1.** Representative male and female Pachón cave karyotypes arranged from

1105 Giemsa-stained mitotic chromosomes (panels A-D) and their corresponding C-banding

1106 patterns (panels A'-D'). B numbers were found to be variable among individuals (from 0 to 3  
 1107 Bs) with all males having a single (panels A-A') or multiple Bs (panels B-B') in most of their  
 1108 metaphases, most females having no B (panels C-C'), and only a few females having rare B  
 1109 positive metaphases (panels D-D') Notice also the lack of C-bands on Bs suggesting that these  
 1110 Pachón cavefish male-predominant Bs are largely euchromatic. Scale bar = 10  $\mu$ m. Male and  
 1111 female numbers referred to Data S1A.  
 1112  
 1113



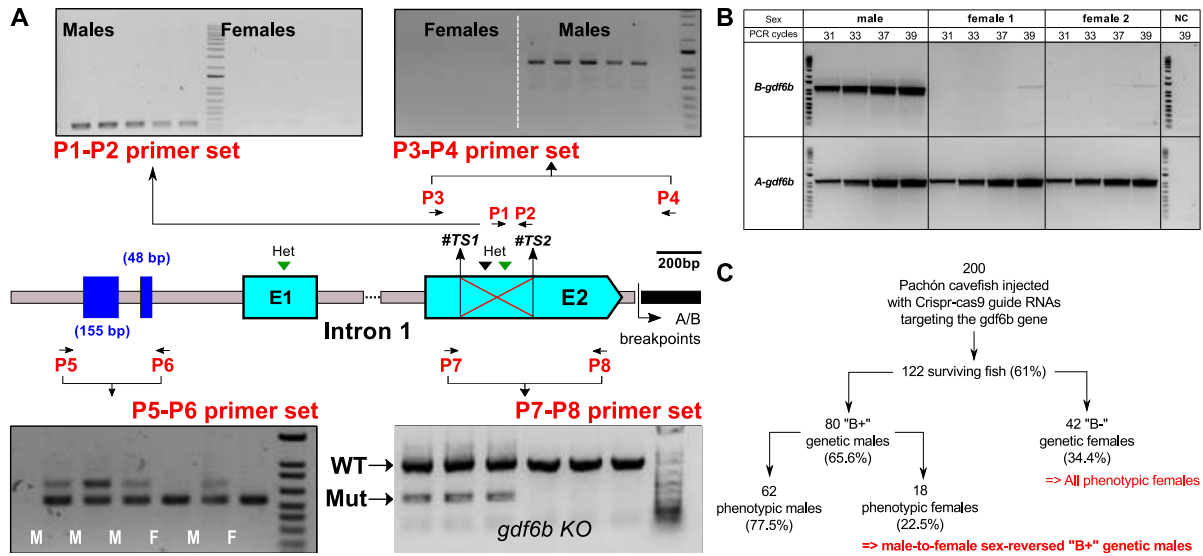
1114 **Figure S2: Genomic repeated elements, *gdf6b* evolution and *gdf6b* sequence alignments.**  
 1115 **Related to Figure 2.** A. Comparison of the GC content and repeated elements in Pachón  
 1116 cavefish B chromosome (B) versus Pachón cavefish A chromosomes. Percentage (in log scale)  
 1117 of GC content (GC level), short interspersed repeated sequences (SINEs), long interspersed  
 1118 nuclear elements (LINEs), long terminal repeats (LTRs), DNA repeat elements (DNAs),  
 1119  
 1120

1121 terminal inverted repeat sequences (TIRs), and satellite DNA (SATs) in the 25 A Pachón  
 1122 chromosomes (boxplots, A) versus Pachón B (black dots, B). **B.** Comparison of the repeat  
 1123 landscapes of the Pachón B chromosome (B), the whole assembly with (whole assembly) and  
 1124 without B and of Scaffold\_25. Color code for repeat elements is provided in the top right inset  
 1125 of the figure. B repeat landscape is different from the whole assembly with or without the B  
 1126 chromosome and to the repeat landscape of scaffold\_25. The B tends to have a higher content  
 1127 of interspersed repeats, mainly due to the expansion of long interspersed nuclear elements  
 1128 (LINEs). Short interspersed repeated sequences (SINEs), long terminal repeats (LTRs), DNA  
 1129 repeat elements (DNAs), and terminal inverted repeat sequences (TIRs). See Data S1D for  
 1130 additional details. **C.** The *B-gdf6b* loci on the Pachón cave *A. mexicanus* B chromosome (B)  
 1131 stemmed from two successive A and B duplications. Schematic representation of the  
 1132 duplication / insertion history of the two *B-gdf6b* loci on the Pachón cave B (HiC\_scaffold\_28)  
 1133 with a two-steps duplication hypothesis scheme suggesting that the *B-gdf6b-1* locus originated  
 1134 from an initial duplication of a 11.4 kb region surrounding the *A-gdf6b* locus and inserted in  
 1135 the B, followed by a second independent duplication of a 21.6 kb region surrounding the *B-*  
 1136 *gdf6b-1* locus that was inserted also in the B. This second independent duplication is probably  
 1137 very recent as the two *B-gdf6b* loci are 99.6 % identical in the 21.6 kb region shared by the two  
 1138 genes. Locations of the duplicated regions are given with respect to the 5'-3' orientation of the  
 1139 *gdf6b* cDNA. The colors of the schematic B fragments depict their different A chromosome  
 1140 origin. **D:** Multiple sequence alignment of Pachón cavefish intron 1 of *A-gdf6b* with *B-gdf6b-*  
 1141 *1* and *B-gdf6b-2*. Sequences were extracted from the whole genome Pachón cavefish assembly  
 1142 with the following coordinates: For *A-gdf6b* = HiC\_scaffold\_3:864791:865845:-, For *B-gdf6b-*  
 1143 *1* = HiC\_scaffold\_28:617028:618422:+ and for *B-gdf6b-2* =  
 1144 HiC\_scaffold\_28:1832027:1833421:-. The percentage of identity between the *A-* and *B-gdf6b*  
 1145 is respectively 1.7 % for intron 1 (18 differences in 1054 bp after gaps and indels collapsed to  
 1146 1 bp) compared to 0.58 % for their proximal promoter (7 differences in 1200 bp after gaps and  
 1147 indels collapsed to 1 bp; proximal promoter defined from the ATG to the 3' end of the adjacent  
 1148 gene, ~ 1400 bp). This could suggest different evolutionary constraints between these two  
 1149 different *gdf6b* regions. **E.** Coding sequence and protein alignments of *A-gdf6b* and *B-gdf6b*.  
 1150 Sequences were aligned with CLUSTALW<sup>S1</sup>. As the *gdf6b-B1* and *gdf6b-B2* are 100%  
 1151 identical from their ATG to STOP codons the alignment only shows differences between *B-*  
 1152 *gdf6b* (*B-gdf6b-1* and *B-gdf6b-2*) and *A-gdf6b* coding sequences (CDS). The three nucleotide  
 1153 variations between the *B-gdf6b* and *A-gdf6b* CDS are boxed (green for nonsynonymous sites  
 1154 and red for synonymous sites) at positions 180 bp, 591 bp and 679 bp positions of the CDS.  
 1155 Regions highlighted in yellow and blue indicated respectively the Pfam “TGF-β propeptide”  
 1156 and “TGF-β-like” domains<sup>S2</sup>. “.”: Identical nucleotides; “\*”: stop codon. **F.** Alignment of  
 1157 nucleotide (*B-gdf6b*) and translated protein sequences (B-Gdf6b) in wild type and one  
 1158 representative example of a mutant male showing a 470 bp deletion in its *B-gdf6b* gene in F0  
 1159 fish in the exon 2 encoding for the Pfam “TGF-β propeptide” (yellow) and the “TGF-β-like”  
 1160 (blue) domains<sup>S2</sup>. The resulting fish displayed a frame-shifted and truncated Gdf6b-B protein  
 1161 with premature stop codon (red). The positions of the guide RNAs selected to inactivate *gdf6b*  
 1162 in Pachón cavefish are boxed in red. Similar 470 bp deletions have been also within the *A-*  
 1163 *gdf6b* gene in other fish.

1164  
 1165



1166



1167

1168 **Figure S3: PCR genotyping of the Pachón cavefish male-predominant B chromosome and**1169 **the *gdf6b* knockout mutant individuals. Related to Figure 4 and STAR Methods. A.**

1170 Absence / presence of the Pachón cavefish B chromosome was detected with different primer

1171 pairs based on differences between the *A-gdf6b* and *B-gdf6b* loci. Three sets of primers (P)1172 were designed with two primer sets designed to amplify specifically the *B-gdf6b* copy based1173 either on a single base variation between the A/B *gdf6b* CDS at position 679 bp (P1-P2 primer1174 set), or based on primers located on both sides of the A/B breakpoints downstream of the *B-*1175 *gdf6b* gene (P3-P4 primer set). The third set of primers (P5-P6 primer set) was designed on1176 gaps/indels variations between *A-gdf6b* and *B-gdf6b* in the proximal promoter of *gdf6b* genes.

1177 Primer sets P1-P2 and P3-P4 produce a single PCR fragment only in B+ individuals, and primer

1178 set P5-P6 amplifies two bands in B+ individuals and only a single band in B- individuals. Gene

1179 knockout (KO) was performed by genome editing using the CRISPR-cas9 method with two

1180 guide RNAs target sites (#TS1 and #TS2) designed in order to target *gdf6b* exon 2 (E2). KO

1181 individuals were genotyped using primers (P7-P8 primer set) flanking the 2 target sites that

1182 induced a 470 bp deletion in *gdf6b* mutant individuals (Mut) compared to the wild type (WT)1183 *gdf6b* sequence. **B.** Increasing PCR cycle numbers allows the detection of a faint PCR fragment

1184 specific to the B chromosome in Pachón cavefish females. PCRs were carried out in one male

1185 and two female Pachón cavefish with the protocol described for the P3-P4 primer set and with

1186 increasing PCR cycle numbers. The B chromosome was detected using primers specifically

1187 designed to amplify the *B-gdf6b* loci (primer set P3-P4) and a control was incorporated with1188 primers specifically designed to amplify the *A-gdf6b* locus (primer set P9-P10). NC: PCR1189 negative control. **C.** Numbers of *gdf6b* knockout generated by CRISPR-Cas9 method including

1190 the number of fish injected, and the number and percentage of sex-reversed males obtained (in

1191 bold red type). Out of the 200 micro-injected eggs (at 1 cell stage), 122 adult fishes were

1192 obtained including 80 genetic males and 42 genetic females. Among the 80 genetic males, we

1193 found 62 phenotypic males (77.5%), and 18 phenotypic females (22.5%) displaying a 470 bp

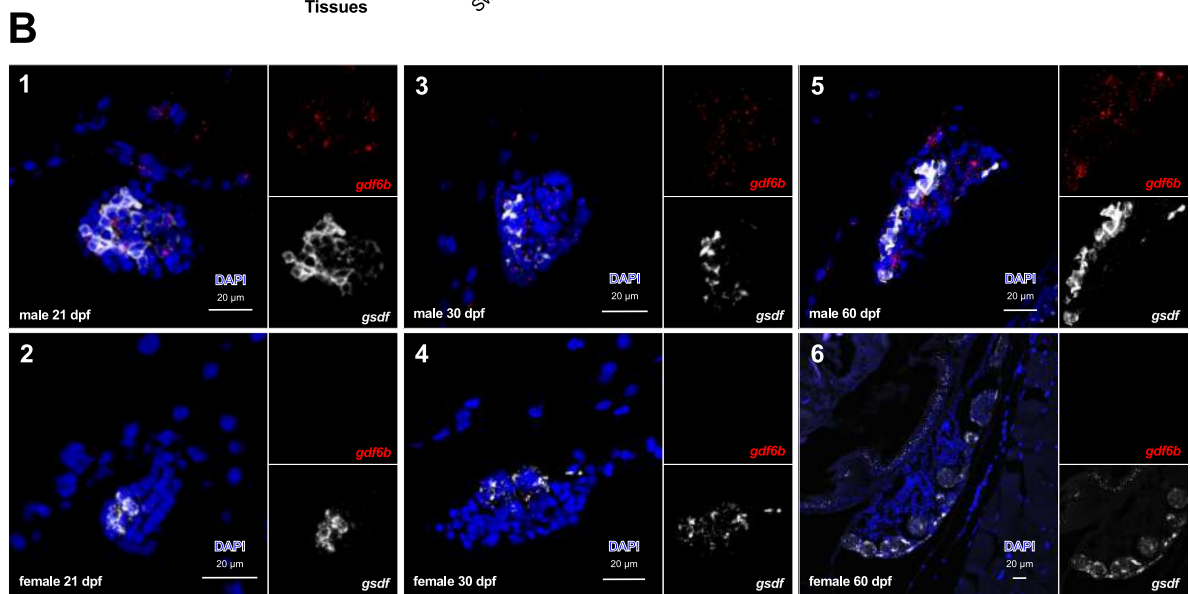
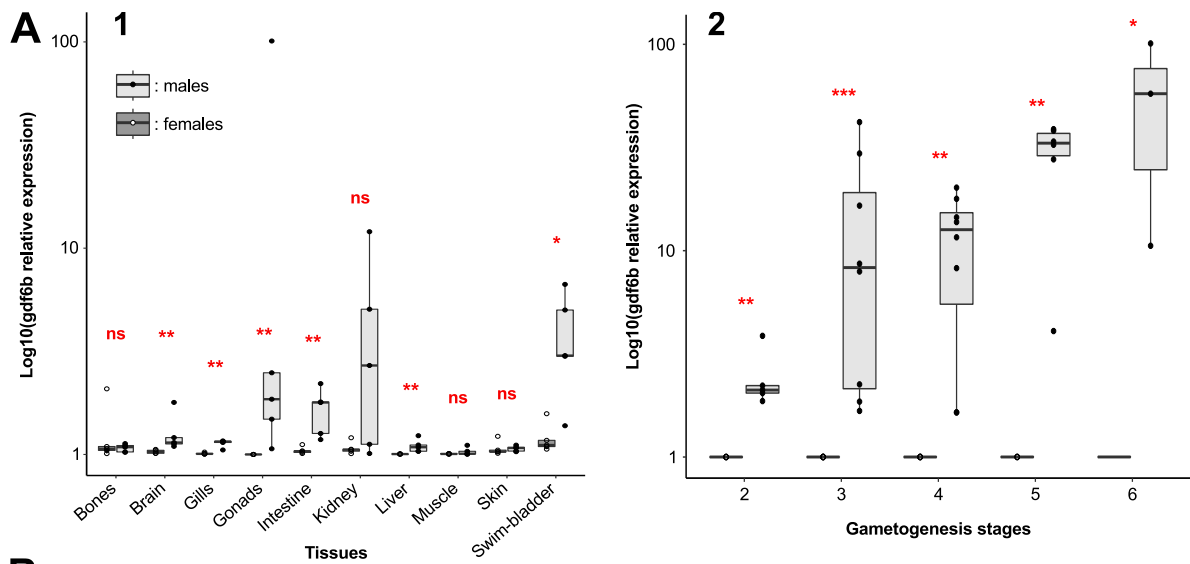
1194 deletion on the exon 2 of their *A-gdf6b* and/or *B-gdf6b* gene.

1195

1196

1197





1198

1199

1200

1201

1202

1203

1204

1205

1206

1207

1208

1209

1210

1211

1212

1213

1214

**Figure S4. Expression patterns of *gdf6b* in adult Pachón cave *Astyanax mexicanus*. Related to Figure 4. A. Expression profiles of *gdf6b* (*A-gdf6b* and *B-gdf6b*) in different adult tissues (A1) in males (light grey) and females (dark grey) and during male (light grey) and female (dark grey) gametogenesis (A2). Gametogenesis stages 2 to 6 were defined as previously described<sup>S3</sup>. Results are presented as boxplots with individual expression values displayed as dots, the expression median as a line, and the box displaying the first and third quartiles of expression. Statistical significance between males and females were tested with the Wilcoxon Rank Sum Test (Wilcoxon-Mann-Whitney Test) and significant differences are \*\*\* = P < 0.01; \*\* = P < 0.01; \* = P < 0.05. B. Gonadal expression of *gdf6b* (in red) and the Sertoli and granulosa supporting cell marker *gsdf* (in white) in male (B1, B3 and B5) and female (B2, B4 and B6) differentiating gonads. At all stages i.e., 21-, 30- and 60-days post-fertilization (dpf) *gdf6b* is specifically expressed in male gonads with no strict colocalization with *gsdf* in males. Nuclei were stained with DAPI (in blue). Scale bar = 20 μm.**

1215 **SUPPLEMENTAL REFERENCES**

1216 S1. Higgins, D.G., and Sharp, P.M. (1988). CLUSTAL: a package for performing multiple  
1217 sequence alignment on a microcomputer. *Gene* 73, 237–244.

1218 S2. El-Gebali, S., Mistry, J., Bateman, A., Eddy, S.R., Luciani, A., Potter, S.C., Qureshi, M.,  
1219 Richardson, L.J., Salazar, G.A., Smart, A., et al. (2019). The Pfam protein families database  
1220 in 2019. *Nucleic Acids Res* 47, D427–D432.

1221 S3. Imarazene, B., Beille, S., Jouanno, E., Branthonne, A., Thermes, V., Thomas, M., Herpin,  
1222 A., Rétaux, S., and Guiguen, Y. (2021). Primordial Germ Cell Migration and Histological  
1223 and Molecular Characterization of Gonadal Differentiation in Pachón Cavefish *Astyanax*  
1224 *mexicanus*. *Sex Dev*, 1–18.

1225

1226